



Molecular cloning, expression and docking studies of *serine protease (SerPr)* and *metalloprotease (MetPr)* of novel *Streptomyces werraensis* KN23 for keratinase activity improvement

Nagwa M. Abd El-Aziz¹, Bigad E. Khalil¹ and Nora N. El-Gamal²

¹Microbial Genetics Department, Biotechnology Research institute, National Research Centre, 33 El Buhouth St., Postal code 12622, Dokki, Cairo, Egypt.

²Microbial Chemistry Department, Biotechnology Research institute, National Research Centre, 33 El Buhouth St., Postal code 12622, Dokki, Cairo, Egypt.

Received: 30 Jan. 2024

Accepted: 07 Mar. 2024

Published: 15 April 2024

ABSTRACT

Because keratinases can break down keratin, keratinases have potential uses in biotechnology. *Streptomyces* appears to be one of the primary providers of these enzymes, yet there are still few complete genome sequences of these microorganisms. This research focuses on isolation the gene encoding *serine protease (SerPr)* and *metalloprotease (MetPr)*, consisting of 3318 and 1119 bp nucleotides (encoding 1105 and 372 amino acids, respectively), from novel *Streptomyces werraensis* KN23 and mutant *Streptomyces werraensis* SA27, the specimen was subjected to isolation, sequencing, and then submitted to the NCBI GenBank database, where it was assigned accession numbers. The structural integrity of the protein model was confirmed by validating its 3D conformation using Ramachandran's plot, which indicated that residues were in the most favourable region for *S. werraensis* KN23 and mutant *Streptomyces werraensis* SA27, respectively. Three amino acids substitution was observed in the *SerPr* protein, and two amino acids substitution variations in *MetPr* protein of the mutant strain SA27. Docking studies revealed optimal binding affinities of the *serine protease (SerPr)* and *metalloprotease (MetPr)* with beta-keratin for *S. werraensis* KN23 and its mutant *Streptomyces werraensis* SA27, respectively. Molecular cloning and expression of the mutant *Streptomyces werraensis* SA27 *serine protease (SerPr)* and *metalloprotease (MetPr)* genes in *E. coli* DH5 α resulted in a recombinant *E. coli* DH5 α pGEM-T-*SerPr* and *E. coli* DH5 α pGEM-T-*MetPr* significantly higher keratinase activity 193.25 and 211.32 U/mL, compared to the mutant *S. werraensis* SA27, which exhibited an activity of 106.92 U/ml. These results suggest that the use of *Streptomyces werraensis* KN23 for keratinase production seems to be very promising, since it has a diverse array of commercial uses, including animal nutrition, the leather sector, and cosmetics.

Keywords: *serine protease (SerPr)*, *metalloprotease (MetPr)*, *Streptomyces werraensis*, modeled structure 3D, Molecular docking, Molecular cloning.

1. Introduction

In 2019, the processing of poultry resulted in the production of almost 4.7 million tons of chicken feathers, according to estimations by Alexandratos and Bruinsma (2012) and Li *et al.* (2020). Category 3 animal byproducts include keratinous residues such as chicken feathers that are produced by poultry processing factories and abattoirs, indicating that they do not provide any danger to people or other animals, or the environment, according to Verma *et al.* (2017). Therefore, they can be viewed as a rich source of protein or amino acids for creative upcycling approaches with the hope of finding usage in a variety of products, including but not limited to feed, fertilizers, and cosmetics (Callegaro *et al.*, 2019). The sulfur-containing amino acid cysteine and other sulfur-containing amino acids like glycine, proline, and arginine give keratinous materials their characteristic properties. They also

Corresponding Author: Nagwa M. Abd El-Aziz, Department of Microbial Genetics, National Research Centre, Dokki, Giza, 12622, Egypt. E-mail: nagwamkh@gmail.com

include high concentrations of the amino acids valine, leucine, and threonine. The major reason for keratin's compact structure and great stability is that cysteine residues inside and between keratin polypeptides create disulfide bridges (Callegaro *et al.*, 2019). Due to its insolubility, keratin must undergo partial or total disintegration to enable viable biorefinery choices because it includes protein and amino acids. Two separate forms of keratin, α -keratin and β -keratin, may be identified based on its secondary structure. The mammalian epidermal materials, often referred to as wool, hair, and horn, are the main sources of α -keratin, whereas birds and reptiles, specifically chicken feathers and reptile scales, are the main sources of β -keratin. Unlike when other natural polymers like collagen, starch, and chitosan are extracted, dissolving and extracting keratin is a challenging procedure. Therefore, the utilization of reasonably quick and affordable extraction-decomposition techniques is essential for the widespread usage of keratin. Physical, chemical, physical-chemical, and biological approaches are all now used for extraction (Shavandi *et al.*, 2017). Nevertheless, the manufacturing process of keratin hydrolysates usually requires the use of elevated temperatures, these causes the hydrolysates' nutritional value to drop because heat-sensitive amino acids like methionine, lysine, and tryptophan are broken down (De Oliveira Martinez *et al.*, 2020). An alternative method involves using keratinolytic microorganisms or, perhaps more effective, targeted keratinases produced by microbes that can catalyse the biodegradation of keratin.

Keratin can be broken down by keratinases, a group of hydrolytic enzymes (EC 3.4.-.-). Keratinolytic enzymes are produced by a variety of bacteria that may be found in water, soil, and materials that are rich in keratin. Some bacteria, such *Stenotrophomonas maltophilia*, *Bacillus subtilis*, and *Bacillus licheniformis*, generate keratinases. *Streptomyces fradiae* and *Streptomyces albidoflavus* are two different actinobacteria that produce keratinases. The keratinase-producing fungus that are most often seen are *Microsporium canis* and *Trichophyton rubrum*. A number of scholarly analyses (Intagun and Kanoksilapatham, 2017; Verma *et al.*, 2017) Provide detailed information on where keratinolytic bacteria came from, and what circumstances are best for fermenting keratinase, methods for measuring keratinase activity, and the characteristics of keratinases. Keratinases are categorized into the serine- and metalloprotease families by the protease family database (MEROPS), using known keratinases as a basis (De Oliveira Martinez *et al.*, 2020). S8 is the principal family of keratinases, and subtilisin subfamily members in particular show keratinolytic activity. There has been talk in the scientific community about how many new protease families have enzymes that can break down keratin. An example of this is the catalytic breakdown of pig bristle keratin by a complex including enzymes from the S8 family as well as proteases from the M28 and M3 families, which are secreted by the non-pathogenic fungus *Onygena corvina* (Huang *et al.*, 2015). The keratin-degrading activity of additional fungal proteases from the M36, S9, and S10 families will be discussed subsequently (Mercer and Stewart, 2019). Therefore, the effectiveness of enzymatic degradation of keratin may be enhanced by strategically combining keratinases from several protease families. In addition, there are additional proteases, such as disulfide reductase (e.g. cysteine dioxygenase (Kasperova *et al.*, 2013), additional enzymes, such as lytic polysaccharide monoxygenases (LPMOs) and thioredoxin-disulfide reductase (Lange *et al.*, 2016). Some enzymes involved in lipoprotein signaling or fatty acid breakdown have also been suggested as enzymes that might help in biocatalytic keratin degradation (Lee *et al.*, 2015b). Although researchers have long been interested in microbial and enzymatic keratin degradation, current overviews often merely summarize keratinase data without delving into great detail on the specifics of the enzymatic action with regard to substrate structure and evaluation technique. Further, a discussion of additional enzymes that might be involved in keratin degradation, a current classification of keratin-degrading enzymes into the protease family, and potential activity synergies are not yet accessible.

Presently, the primary focus of molecular investigations and characterizations of keratinases is centered on the isolation of these enzymes from diverse bacteria and their subsequent introduction into *E. coli* hosts. Due to its broad utilization as an expression host for recombinant keratinase, *E. coli* is considered the most extensively researched model microorganism. Compared to utilizing the native host, there are a number of benefits to expressing keratinase in *E. coli*. To start with, it opens the door to optimizing recombinant keratinase synthesis using different strains of *E. coli*. Second, to ease purification operations and regulate recombinant keratinase induction, a variety of vectors may be used. Thirdly, auto-inducible, constitutive, or inductive promoters may be used to modify the expression of recombinant keratinases. The last step is to use rational design to improve the cloned

recombinant keratinase's properties even more (Yahaya *et al.*, 2021). Due to its genetic adaptability and the abundance of expression vectors, *E. coli* is the primary choice as a heterologous host for expressing recombinant keratinase. The majority of molecular investigations on recombinant keratinases used the pET vector to facilitate keratinase expression in *E. coli* (Gupta *et al.*, 2017).

This research focuses on the *serine protease* and *metalloprotease*-encoding gene, which was isolated, sequenced, and deposited in the NCBI GenBank database. The 3D structure of the *serine protease* (*SerPr*) and *metalloprotease* (*MetPr*) proteins was modelled and validated using Ramachandran's plot, with template proteins from *Streptomyces werraensis* JCM 4860, *Streptomyces werraensis* KN23, and mutant *Streptomyces werraensis* SA27. In addition, molecular docking experiments were performed to provide a better understanding of the protein's binding properties. Expression of the *serine protease* and *metalloprotease*-encoding gene from mutant *Streptomyces werraensis* SA27 in *E. coli* *DH5a*, aiming to enhance keratinase activity.

2. Materials and Methods

2.1. Plasmids, Reagents, Media and Strains

Streptomyces werraensis KN23 (accession no. OK086273) and its mutant *Streptomyces werraensis* SA27, which might effectively break down the feathers. The samples were kept in our laboratory according to the specified instructions (Abd El-Aziz *et al.*, 2023a). *E. coli* *DH5a* was cultivated at a temperature of 37 degrees Celsius for a duration of 12 to 18 hours in either Luria-Bertani (LB) broth or low-salt LB medium. The solution has the following concentrations (g/L): NaCl, 10.0; yeast extract, 5.0; and tryptone, 10.0. Plate count (P.C.) agar medium (Himedia, West Chester, Pennsylvania, USA) was used for actinomycetes growth. The following components were included in the basic medium used to isolate and ferment that degrade feathers: NaCl (0.5), KH₂PO₄ (0.7), K₂HPO₄ (1.4), MgSO₄ (0.1), and feathers (10), with a pH of 7.2 (Cai *et al.*, 2008). A plasmid called pGEM-T Easy-cloning was purchased from Promega Co. in Madison, WI, USA. It has 3015 base pairs and was manufactured by ampicillin Amp^r. Both wild-type *Streptomyces werraensis* KN23 and its mutant SA27 strains have their genomic DNA extracted. With the use of a genomic DNA isolation kit made in Taoyuan, Taiwan by GeneDireX, Inc. The QIA prep spin miniprep kit was used to extract plasmid DNA from *E. coli* *DH5a*. Both NEB in the US and TaKaRa in China supplied the T4 DNA ligase.

2.2. *Serine protease* (*SerPr*) and *metalloprotease* (*MetPr*) encoding gene amplification

Initially, the primers designed for the *serine protease* (*SerPr*) and *metalloprotease* (*MetPr*) genes of *Streptomyces werraensis* JCM 486, the design of the product was based on its DNA sequence. Novel genomic DNA was isolated *S. werraensis* KN23 strain (NCBI Accession No.OK086273) and its mutant *Streptomyces werraensis* SA27 as reported by Abd El-Aziz *et al.* (2023a), using a genomic DNA isolation kit (GeneDireX, Inc., Taoyuan, Taiwan) and used for amplifying the *serine protease* and *metalloprotease* genes. By using primers that have been specifically developed according to the significant similarity in DNA sequences of *serine protease* (*SerPr*) and *metalloprotease* (*MetPr*) genes among *S. werraensis* strains, the specific primers used were as follows: forward primer *SerPr*-F (5'-ATGACCAACTCCCCGAGC-3') and reverse primer *SerPr*-R (5'-CTACGGGACGACCTTCTCGATC-3'), forward primer *MetPr*-F (5'-ATGGTCGCGGGCAGTGACA-3'), and reverse primer *MetPr*-R (5'-CTACAGCGTGCGCACCCC-3') using Primer3 software. The PCR was carried out using a GeneAmp PCR System 2400 thermal cyclor from PerkinElmer in Norwalk, Connecticut, USA, with 100 ng of genomic DNA in a 100 µl reaction containing master mix (TIANGEN, Beijing, China) and 5 µM primers (Gupta *et al.*, 2017). Starting with a denaturation at 95°C for 5 minutes, the thermal protocol went into annealing at 55°C for 1 minute, extension at 72°C for 2 minutes per kilobase pair (kbp), and finally, an extension at 72°C for 3 minutes. The total number of cycles was 35. A FavorPrep gel purification kit (FAVORGEN, Biotech Corp., Ping Tung, Taiwan) was used to elute the amplified genes before sending them out for sequencing, after electrophoresis on a 1% agarose gel, the PCR findings were analyzed (Ouled-Haddar *et al.*, 2010).

2.3. Bioinformatics analysis

By use the online translation tool ExPASy (<http://web.expasy.org/translate>), the *serine protease* (*SerPr*) and *metalloprotease* (*MetPr*) The protein sequence was acquired from the experimentally ascertained data *SerPr* and *MetPr* protein gene of *S. werraensis* KN23 and mutant *S. werraensis* SA27. The inferred amino acids were examined using the NCBI protein blast (<http://BLAST:> (Basic Local Alignment Search Tool (nih.gov))). Blast queries the protein sequence database without duplicates, and considers hits with identical sequences as matches. Protein sequences underwent Multiple Sequence Alignment (MSA) using the PRALINE web resource portal (<http://www.ibi.vu.nl/programs/pralinewww/>) (Mei *et al.*, 2013; Eswar *et al.*, 2006). The online PDBsum service was used to do secondary structure prediction of the *SerPr* and *MetPr* proteins PDBsum home page (ebi.ac.uk). Yang and Yang (2015). Cluster analysis (phylogenetic tree) of *S. werraensis SerPr* and *MetPr* protein sequence analysis was conducted using the MEGAX program (MEGA-software [ILRI Research Computing] (cgjar.org)).

2.4. Homology modelling, validation, and binding pocket prediction of *SerPr* and *MetPr*

In order to forecast the tertiary configuration of *SerPr* and *MetPr* protein, ROSETTA (rosetta.bakerlab.org) was used (Kathwate 2020; Heo *et al.*, 2013). Five models were produced, and the model with the highest confidence score (C-score, a metric indicating the accuracy of the anticipated model) was selected as the best (Sahi *et al.*, 2012; Singh and Muthusamy, 2013; Webb and Sali 2016). The C-score typically ranges from zero to one. An obvious relationship exists between the C-score and structural quality. Among the five generated models, an optimized *SerPr* and *MetPr* homology model was constructed using the "DOPE profile" options. The optimal validation framework for *SerPr* and *MetPr* proteins was verified using the SAVES v6.0 (structure analysis and verification server version 6) web tool (<http://SAVESv6.0> - Structure Validation Server (ucla.edu)) as well as the *ProSA* server. A total of five programs make up SAVES v6.0, and their purpose is to evaluate the protein structure's overall integrity. Out of the five tools we employed, two stood out: VERIFY-3D, which analyzed the three-dimensional sequence profiles of protein models, and PROCHECK, which evaluated the structure using the Ramachandran plot (Patni *et al.*, 2021; Beg *et al.*, 2018). Using the "PyMol" software developed by DeLano Scientific LLC, a stereo picture of the *SerPr* and *MetPr* model was created to display the surface groove structure (Gupta *et al.*, 2017). The Site-Map module is a component of the deepsite/playmolecule online tool (<http://DeepSite:> a binding pocket predictor using neural-networks [WEB APP] (playmolecule.com)), the *SerPr* and *MetPr* protein and ligand beta keratin were subjected to binding site predictions using the aforementioned method (Kesharwani and Misra 2011). In order to identify potential binding sites of amino acids, we considered physical properties like size, degree of exposure or enclosure, hydrophobicity or hydrophilia, tightness, and hydrogen-bonding potential (Banerjee *et al.*, 2014).

2.5. Molecular docking studies

The MOE program was used to process the 3D structure of the *SerPr* and *MetPr* proteins (Molecular Operating Environment (MOE) | MOEsaic | PSILO (chemcomp.com)), Decanting the concentration of ions, water molecules, and present ligands. The receptor molecule was functionalized with hydrogen atoms by means of PyMOL (PyMOL | pymol.org). The beta keratin substrate ligand was created in pdb format using MOE and PyMOL; its PubChem CID is 395651 and its PF02422 code is beta keratin. The HDock online program was used to perform protein-protein docking investigations ([http:// HDock](http://HDock) Server (hust.edu.cn)) (Degryse *et al.*, 2008; Patni *et al.*, 2021), in order to learn how beta-keratin interacts with *SerPr* and *MetPr*. Docking was the reason for saving the macromolecule file in PDB format (Gupta *et al.*, 2017; Banerjee *et al.*, 2014 and Sahi *et al.*, 2012).

2.6. Cloning and expression of *SerPr* and *MetPr* encoding genes

The amplified product *SerPr* and *MetPr* of mutant SA27 (Abd El-Aziz *et al.*, 2023a) The pGEM®-T Easy cloning vector was used for ligation cloning using a kit from Promega Co., located in Madison, WI, USA. The insert was placed into the appropriate locations of the vector. To generate the recombinant plasmid, a ligation procedure is performed with the enzyme T4 ligase. The DNA that had been ligated (20 µl) was combined with 0.1 ml of recently generated competent cells, which had a

transformation efficiency of 2.98×10^5 colony-forming units per microgram of DNA (Barman *et al.*, 2014). The recombinant plasmid was introduced into *E. coli DH5a* cells by the heat shock technique, followed by incubation at 37°C for 1 hour. Following incubation, the samples were spread onto LB agar plates supplemented with 0.5 mM IPTG, 50 µg/mL ampicillin, and 40 µg X-gal. The plates were then incubated overnight at 37°C. Positive colonies were identified using the blue-white screening method. Colonies of *SerPr* and *MetPr* were streaked once again on a suitable plate containing antibiotics and then incubated at a temperature of 37 degrees Celsius for a period of 16 to 20 hours. The extracellular expression of *SerPr* and *MetPr* activity was measured in positive colonies at 37°C (Kesharwani and Misra, 2011; Froger and Hall, 2007; Gupta *et al.*, 2017; Singh *et al.*, 2012; and Mei *et al.*, 2013). A 50 mL culture of *E. coli DH5a* cells, transformed with plasmids *pGEM-T-SerPr* and *pGEM-T-MetPr*, were prepared by inoculating overnight-grown single colonies into Luria-Bertani (LB) broth medium supplemented with ampicillin (50 µg/mL). The culture was then incubated at 37°C with shaking for 16 hours. The mature culture was subjected to centrifugation at a speed of 4000 revolutions per minute for a duration of 10 minutes at a temperature of 4 degrees Celsius. Next, the liquid portion above the sedimented cells was removed, and the solid cell material was used for extracting the modified plasmid DNA molecule using the QIA prep spin miniprep kit from Germany, following the instructions provided by the manufacturer (Mei *et al.*, 2013; Maha, 2017). The colonies that underwent transformation with the plasmid containing the *SerPr* and *MetPr* gene (*pGEM-T-SerPr* and *pGEM-T-MetPr*) were examined using colony PCR. This screening process included the use of particular primers for the *SerPr* and *MetPr* genes, and the same PCR conditions that were used for amplifying these genes (Mei *et al.*, 2013).

2.7. Preparation of crude enzyme extract and keratinase enzyme assay

The assessment of keratinolytic activity included the use of soluble keratin (0.5%, w/v) as the substrate. This substrate was derived from white chicken feathers, following the method outlined in the reference (Wawrzkiwicz *et al.*, 1987) Feathers from indigenous chickens weighing 10 grams were obtained from several local poultry stores in Cairo, Egypt. The feathers were subjected to treatment with Dimethyl sulfoxide (DMSO), later on, after heating, the mixture was precipitated with cold acetone. We washed, dried, and dissolved the precipitate in sodium hydroxide solution. Using a Tris-HCl buffer (pH 8.0), the solution's pH was adjusted and diluted (Cai *et al.*, 2008). A particular strain was added to a fermentation medium that had been supplemented with 1% feather to stimulate the production of keratinase. For a quantitative keratinase test, the enzyme-containing supernatant was collected. By using a keratin solution as the substrate, the activity of the enzyme was measured, following the procedure outlined by Cai *et al.* (2008). Specifically, the diluted crude enzyme (1.0 ml) was incubated with keratin solution (1 ml) at 50°C for 10 minutes, and the reaction was stopped with trichloroacetic acid (TCA). After centrifugation, the absorbance of the supernatant was measured at 280 nm against a control. An increase in corrected absorbance was used to determine keratinolytic activity of 280 nm (A_{280}) at a rate of 0.01 per minute. The activity (U/ml) was calculated using the equation: $U = 4 \times n \times A_{280} / (0.01 \times 10)$, where n is the dilution rate (Gradisar *et al.*, 2005).

3. Results and Discussion

3.1. Serine protease (*SerPr*) and metalloprotease (*MetPr*)-encoding genes amplification and alignment in Genbank (Blast)

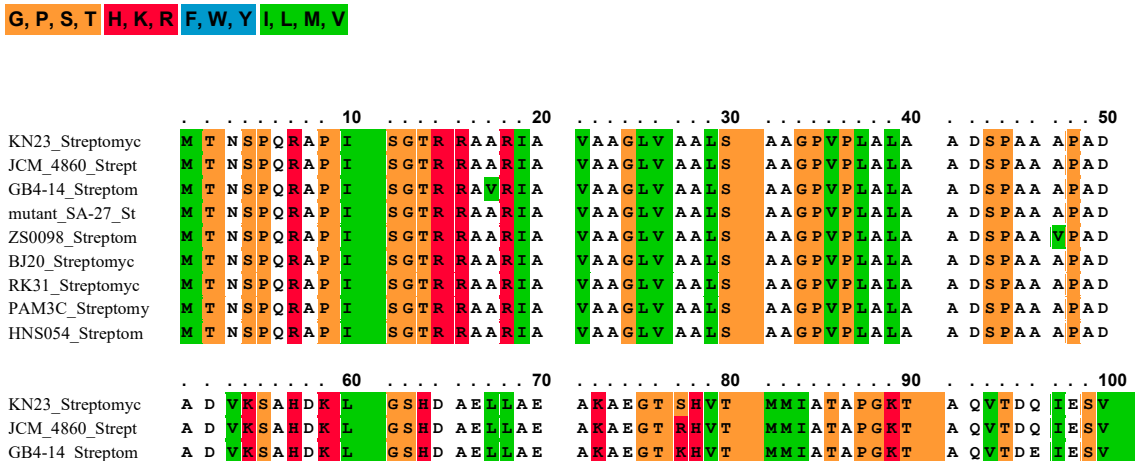
In a previous study conducted by Abd El-Aziz *et al.* (2023a) novel actinomycetes *S. werraensis* KN23 strain and mutant *S. werraensis* SA27 were isolated from different farms in Cairo, Egypt. The designed primers were for the serine protease (*SerPr*) and metalloprotease (*MetPr*). The genes were successfully enhanced and sequenced. After that, we used BLAST to compare the obtained sequence to known sequences in the NCBI database. The analysis revealed *SerPr* and *MetPr* have an open reading frame (ORF) of 3318 and 1119 bp, respectively, in line with the anticipated duration of the *SerPr* and *MetPr* genes in *S. werraensis* KN23 and mutant *S. werraensis* SA27, at the first time. These genes sequence encodes a protein comprising 1105 and 372 amino acids, respectively. The comparison also showed that the *SerPr* and *MetPr* genes and translated proteins from *S. werraensis* KN23 and mutant *S. werraensis* SA27 shared 99% similarity with the *SerPr* and *MetPr* genes of *S. werraensis* strain JCM 4860. Consequently, the obtained sequence for the *SerPr* and *MetPr* genes in *S. werraensis* KN23 and mutant *S. werraensis* SA27 was submitted to the NCBI database with the

accession numbers OR464168, OR464169 for *SerPr*, and OR464170, OR464171 for *MetPr*, for *S. werraensis* KN23 and mutant *S. werraensis* SA27, respectively. Subsequently, Proteins *SerPr* and *MetPr* were represented by their respective amino acid sequences, which were generated from the nucleotide sequences of the genes. We used the UniProt protein database to find three more *SerPr* and *MetPr* sequences that corresponded with the amino acid sequence. Additionally, the InterProScan server (EMBL) identified amino acid 1-1105 and 1-372 residues as belonging to the *SerPr* and *MetPr* families.

In a related studies of according to Gupta *et al.* (2017), *Bacillus subtilis* RSE163 contains the keratinase (*ker*) gene, which codes for 447 amino acids and comprises 1342 base pairs of nucleotides. This gene was successfully amplified using primers that are unique to it. While targeting the *kerA* gene—which codes for the keratinase enzyme—in a polymerase chain reaction, *Bacillus licheniformis* MZK-05 produced an amplicon of 1,156 bp (Nahar *et al.*, 2016). Making use primers that are particular to genes, (Peng *et al.*, 2020). There was successful reporting of keratinase gene amplification from *Bacillus licheniformis* BBE11-1. Amplification of the *Bacillus licheniformis* KRLr1 keratinase gene to 1,050 kb is now associated with the accession number MT482301.1 in the NCBI database by Rahimnahal *et al.* (2023). Extracts of wild-type keratinase (*KerS*) genes were used for amplification (S1, S13, S15, S26, and S39) and their corresponding mutants (S1ems, S13uv, S13uv+ems, S15ems, S26uv, and S39ems) according to Almahasheer *et al.* (2022). It's interesting to note that the *B. cereus* group's Four types of serine proteases: keratinase, thermophilic, alkaline, and thermophilic all had 95.5–100% similarity with the keratinase *KerS* gene. The *kerT1* gene (1170 bp) from the feather-degrading bacteria *Thermoactinomyces sp.* YT06 was effectively amplified, according to Wang *et al.* (2019) publication. In a related study of Abd El-Aziz *et al.* (2023b) The *Metalloprotease (MetPr)* gene was discovered in a new strain of *Pichia kudriavzevii* YK46, subsequent to which its sequence was determined and it was deposited into the NCBI GenBank database with the identifier OQ511281. (Abd El-Aziz *et al.*, 2023c) extracted, sequenced, and uploaded to NCBI with accession codes OQ283005 and OQ283006, respectively, are the *endo-polygalacturonase PGI* gene sequences from *Rhodotorula mucilaginosa* PY18 and mutant *Rhodotorula mucilaginosa* E54. This is the first time these sequences have been published.

3.2. Serine protease (*SerPr*) and metalloprotease (*MetPr*) multiple sequence alignment (MSA) and active site prediction

The multiple sequence alignment analysis revealed the presence of nine consensus regions in the *serine protease (SerPr)* sequence. Among them, the sequence of *S. werraensis* KN23 and mutant *S. werraensis* SA27 exhibited the highest degree of similarity to the *serine protease (SerPr)* sequence of *S. werraensis* JCM 4860, indicating their close relationship within the *Streptomyces* genus. Notably, investigations focused on the active site of the *serine protease (SerPr)* enzymes from *S. werraensis* KN23 and mutant *S. werraensis* SA27, which revealed the presence of seven amino acids substitutions ARG251, PRO252, TYR264, THR991, SER1009, SER246 and TRP376 at specific positions, as depicted in Figure 1.



mutant_SA-27_St	A D V K S A H D K L G S H D A E L L A E A K A E G T S H V T M M I A T A P E K T A Q V T D Q I E S V
ZS0098_Streptom	A D V K S A H D K L G S H D A E L L A E A K A D A G A K H V T M M I A T A P G K T A Q V T E E I E S V
BJ20_Streptomyc	A D V K S A H D K L G S H D A E L L A E A K A G G A K H V T M M I A T A P G K T A Q V T E E I E S V
RK31_Streptomyc	A D V K S A H D K L G S H D A E L L A E A K A D A G A K H V T M M I A T A P G K T A Q V T E E I E S V
PAM3C_Streptomyc	A D V K S A H D K L G S H D A E L L A E A K A D A G A K H V T M M I A T A P G R T A Q V T E E I E S V
HNS054_Streptom	A D V K S A H D K L G S H D A E L L A E A K A D A G A K H V T M M I A T A P G R T A Q V T E E I E S V

KN23_Streptomyc 110 120 130 140 150
JCM_4860_Strept	K G A S V G R S D D K L G Y V R A T V P T G K A D A A I A A A T K L S S V H G V D L R D E I P L D D
GB4-14_Streptom	K G A S V G R S D D K L G Y V R A T V P T G K A D A A I A A A T K L S S V H G V D L R D E I P L D D
mutant_SA-27_St	K G A S V G R S D D K L G Y V R A T V P T G K A D A A I A A A T K L S S V H G V D L R D E I P L D D
ZS0098_Streptom	R G A S V G R S D D K L G Y V R A T V P T G K A D A A I A A A T K L S T V H G V D L R D E I P L D D
BJ20_Streptomyc	R G A S V G R S D D K L G Y V R A T V P T G K A D A A I A A A T K L S T V H G V D L R D E I P L D D
RK31_Streptomyc	R G A S V G R S D D K L G Y V R A T V P T G K A D A A I A A A T K L S T V H G V D L R D E I P L D D
PAM3C_Streptomyc	R G A S V G R S D D K L G Y V R A T V P T G K A D A A I A A A T K L S T V H G V D L R D E I P L D D
HNS054_Streptom	R G A S V G R S D D K L G Y V R A T V P T G K A D A A I A A A T K L S T V H G V D L R D E I P L D D

KN23_Streptomyc 160 170 180 190 200
JCM_4860_Strept	P T P A G D T T K A A K G K G G S A K S Y P A P D R K T P A K N P Y N P S F E T G A V D F V K K N P
GB4-14_Streptom	P T P A G D T T K A A K G K G G S A K S Y P A P D R K T P A K N P Y N P S F E T G A V D F V K K N P
mutant_SA-27_St	P T P A G D T T K A A K G K G G S A K S Y P A P D R K T P A K N P Y N P S F E T G A V D F V K K N P
ZS0098_Streptom	P T P A G D T T K A A K G K G K S V K S Y P A P D R K T P A K N P Y N P S F E T G A V D F V K K N P
BJ20_Streptomyc	P T P A G D T T K A A K G K G K S V K S Y P A P D R K T P A K N P Y N P S F E T G A V D F V K K N P
RK31_Streptomyc	P T P A G D T T K A A K G K G K S V K S Y P A P D R K T P A K N P Y N P S F E T G A V D F V K K N P
PAM3C_Streptomyc	P T P A G D T T K A A K G K G K S V K S Y P A P D R K T P A K N P Y N P S F E T G A V D F V K K N P
HNS054_Streptom	P T P A G D T T K A A K G K G K S V K S Y P A P D R K T P A K N P Y N P S F E T G A V D F V K K N P

KN23_Streptomyc 210 220 230 240 250
JCM_4860_Strept	K A D G R G V T I G I L D S G V D L G H P A L Q R T T T G E R K I V D W V T A T D P I V D S D Q T W
GB4-14_Streptom	K A D G R G V T I G I L D S G V D L G H P A L Q R T T T G E R K I V D W V T A T D P I V D S D Q T W
mutant_SA-27_St	K A D G R G V T I G I L D S G V D L G H P A L Q R T T T G E R K I V D W V T A T D P I V D S D Q T W
ZS0098_Streptom	K A D G R G V T I G I L D S G V D L G H P A L Q R T T T G E R K I V D W V T A T D P I V D G D Q T W
BJ20_Streptomyc	K A D G R G V T I G I L D S G V D L G H P A L Q R T T T G E R K I V D W V T A T D P I V D G D Q T W
RK31_Streptomyc	K A D G R G V T I G I L D S G V D L G H P A L Q R T T T G E R K I V D W V T A T D P I V D G D Q T W
PAM3C_Streptomyc	K A D G R G V T I G I L D S G V D L G H P A L Q R T T T G E R K I V D W V T A T D P I V D G D Q T W
HNS054_Streptom	K A D G R G V T I G I L D S G V D L G H P A L Q R T T T G E R K I V D W V T A T D P I V D S D Q T W

KN23_Streptomyc 260 270 280 290 300
JCM_4860_Strept	R P M V N A V S G P A F T Y G G A T W K A P Q G S Y Q V S L F R E S Y T T G G D A A G D A N R D G D
GB4-14_Streptom	R P M V N A V S G P A F T Y G G A T W K A P Q G S Y Q V S L F R E S Y T T G G D A A G D A N R D G D
mutant_SA-27_St	R P M V N A V S G P A F T Y G G A T W K A P Q G S Y Q V S L F R E S Y T T G G D A A G D A N R D G D
ZS0098_Streptom	R P M V N A V S G P A F T Y G G A T W K A P Q G S Y Q V S L F R E S Y T T G G D A A G D A N R D G D
BJ20_Streptomyc	R P M V N A V S G P A F T Y G G A T W K A P Q G S Y Q V S L F R E S Y T T G G D A A G D A N R D G D
RK31_Streptomyc	R P M V N A V S G P A F T Y G G A T W K A P Q G S Y Q V S L F R E S Y T T G G D A A G D A N R D G D
PAM3C_Streptomyc	R P M V N A V S G P A F T Y G G A T W K A P Q G S Y Q V S L F R E S Y T T G G D A A G D A N R D G D
HNS054_Streptom	R P M V N A V S G P A F T Y G G A T W K A P Q G S Y Q V S L F R E S Y T T G G D A A G D A N R D G D

KN23_Streptomyc 310 320 330 340 350
JCM_4860_Strept	T T D V W G V L Y D P A A G T V R V D L N N N Q D F S D D T P M K P Y R D G F Q I G Y F G T D D P K
GB4-14_Streptom	T T D V W G V L Y D P A A G T V R V D L N N N Q D F S D D T P M K P Y R D G F Q I G Y F G T D D P K
mutant_SA-27_St	T T D V W G V L Y D P A A G T V R V D L N N N Q D F S D D T P M K P Y R D G F Q I G Y F G T D D P K
ZS0098_Streptom	T T D V W G V L Y D P A A G T V R V D L N N N Q D F S D D T P M K P Y R D G F Q I G Y F G T D D P K
BJ20_Streptomyc	T T D V W G V L Y D P A A G T V R V D L N N N Q D F S D D T P M K P Y R D G F Q I G Y F G T D D P K
RK31_Streptomyc	T T D V W G V L Y D P A A G T V R V D L N N N Q D F S D D T P M K P Y R D G F Q I G Y F G T D D P K
PAM3C_Streptomyc	T T D V W G V L Y D P A A G T V R V D L N N N Q D F S D D T P M K P Y R D G F Q I G Y F G T D D P K
HNS054_Streptom	T T D V W G V L Y D P A A G T V R V D L N N N Q D F S D D T P M K P Y R D G F Q I G Y F G T D D P K

KN23_Streptomyc 360 370 380 390 400
JCM_4860_Strept	T D V A E R Q P F V V E I R K D V P M D P Y G G D W V G K K A D F V N I G V I E S E H G T H V A G I
GB4-14_Streptom	T D V A E R Q P F V V E I R K D V P M D P Y G G D W V G K K A D F V N I G V I E S E H G T H V A G I
mutant_SA-27_St	T D V A E R Q P F V V E I R K D V P M D P Y G G D W V G K K A D F V N I G V I E S E H G T H V A G I
ZS0098_Streptom	T D V A E R Q P F V V E I R E D V P M D P Y G G D W I G Q K A D F V N I G V I E G S H G S H V A G I
BJ20_Streptomyc	T D V A E R Q P F V V E I R K D V P M D P Y G G D W I G Q K A D F V N I G V I E G S H G S H V A G I
RK31_Streptomyc	T D V A E R Q P F V V E I R E D V P M D P Y G G D W I G Q K A D F V N I G V I E G S H G S H V A G I
PAM3C_Streptomyc	T D V A E R Q P F V V E I R E D V P M D P Y G G D W I G Q K A D F V N I G V I E G S H G S H V A G I
HNS054_Streptom	T D V A E R Q P F V V E I R E D V P M D P Y G G D W I G Q K A D F V N I G V I E G S H G S H V A G I

*

	410	420	430	440	450
KN23_Streptomyc	T A N G L F G G K	M N G A A P G A K L	V S S R A C	T W S G G C T N V A L T E G	M I D L V T K R G V
JCM_4860_Strept	T A N G L F G G K	M N G A A P G A K L	V S S R A C	T W S G G C T N V A L T E G	M I D L V T K R G V
GB4-14_Streptom	T A N G L F G G K	M N G A A P G A K L	V S S R A C	T W S G G C T N V A L T E G	M I D L V T K R G V
mutant_SA-27_St	T A N G L F G G K	M N G A A P G A K L	V S S R A C	T W S G G C T N V A L T E G	M I D L V T K R G V
ZS0098_Streptom	T A N G L F G G R	M N G A A P G A K L	V S S R A C	T W S G G C T N V A L T E G	M I D L V T K R G V
BJ20_Streptomyc	T A N G L F G G R	M N G A A P G A K L	V S S R A C	T W S G G C T N V A L T E G	M I D L V T K R S V
RK31_Streptomyc	T A N G L F G G R	M N G A A P G A K L	V S S R A C	T W S G G C T N V A L T E G	M I D L V T K R G V
PAM3C_Streptomyc	T A N G L F G G R	M N G A A P G A K L	V S S R A C	T W S G G C T N V A L T E G	M I D L V T K R G V
HNS054_Streptom	T A N G L F G G R	M N G A A P G A K L	V S S R A C	T W S G G C T N V A L T E G	M I D L V T K R G V

	460	470	480	490	500
KN23_Streptomyc	D I V N M S I G G L	P A L N D G N N A R	A E L Y T R L I D T	Y G V Q L V I S A G	N S G P G A N T I G
JCM_4860_Strept	D I V N M S I G G L	P A L N D G N N A R	A E L Y T R L I D T	Y G V Q L V I S A G	N S G P G A N T I G
GB4-14_Streptom	D I V N M S I G G L	P A L N D G N N A R	A E L Y T R L I D T	Y G V Q L V I S A G	N S G P G A N T I G
mutant_SA-27_St	D I V N M S I G G L	P A L N D G N N A R	A E L Y T R L I D T	Y G V R L V I S A G	N S G P G A N T I G
ZS0098_Streptom	D I V N M S I G G L	P A L N D G N N A R	A E L Y N R L I D T	Y G V Q L V I S A G	N S G P G A N T I G
BJ20_Streptomyc	D I V N M S I G G L	P A L N D G N N A R	A E L Y N R L I D T	Y G V Q L V I S A G	N S G P G A N T I G
RK31_Streptomyc	D I V N M S I G G L	P A L N D G N N A R	A E L Y N R L I D T	Y G V Q L V I S A G	N S G P G A N T I G
PAM3C_Streptomyc	D I V N M S I G G L	P A L N D G N N A R	A E L Y N R L I D T	Y G V Q L V I S A G	N S G P G A N T I G
HNS054_Streptom	D I V N M S I G G L	P A L N D G N N A R	A E L Y N R L I D T	Y G V Q L V I S A G	N S G P G A N T I G

	510	520	530	540	550
KN23_Streptomyc	D P A L A D K V I S	A G A S V S K E T W	A A N Y G S E V K T	S Y A M M P F S S R	G P R E D G G F T P
JCM_4860_Strept	D P A L A D K V I S	V G A S V S K E T W	A A N Y G S E V K T	S Y A M M P F S S R	G P R E D G G F T P
GB4-14_Streptom	D P A L A D K V I S	V G A S V S K E T W	A A N Y G S E V K T	S Y A M M P F S S R	G P R E D G G F T P
mutant_SA-27_St	D P A L A D K V I S	A G A S V S K E T W	A A N Y G S E V K T	S Y A M M P F S S R	G P R E D G G F T P
ZS0098_Streptom	D P A L A D K V I S	V G A S V S K E T W	A A N Y G S E V K T	K Y A M M P F S S R	G P R E D G G F T P
BJ20_Streptomyc	D P A L A D K V I S	V G A S V S K E T W	A A N Y G S E V K T	K Y A M M P F S S R	G P R E D G G F T P
RK31_Streptomyc	D P A L A D K V I S	V G A S V S K E T W	A A N Y G S A V K T	K Y A M M P F S S R	G P R E D G G F T P
PAM3C_Streptomyc	D P A L A D K V I S	V G A S V S K E T W	A A N Y G S A V K T	K Y A M M P F S S R	G P R E D G G F T P
HNS054_Streptom	D P A L A D K V I S	V G A S V S K E T W	A A N Y G S A V K T	K Y A M M P F S S R	G P R E D G G F T P

	560	570	580	590	600
KN23_Streptomyc	T L T A P G A A I N	T I Q T W L P G A P	V A E A G Y S L P A	G Y G M I Q G T S M	A S P Q A A G A S A
JCM_4860_Strept	T L T A P G A A I N	T I Q T W L P G A P	V A E A G Y S L P A	G Y G M I Q G T S M	A S P Q A A G A S A
GB4-14_Streptom	T L T A P G A A I N	T I Q T W L P G A P	V A E A G Y S L P A	G Y G M I Q G T S M	A S P Q A A G A S A
mutant_SA-27_St	T L T A P G A A I N	T I Q T W L P G A P	V A E A G Y S L P A	G Y G M I Q G T S M	A S P Q A A G A S A
ZS0098_Streptom	T L T A P G A A V N	T I Q T W L P G A P	V A E A G Y S L P A	G Y G M I Q G T S M	A S P Q A A G A S A
BJ20_Streptomyc	T L T A P G A A V N	T I Q T W L P G A P	V A E A G Y S L P A	G Y G M I Q G T S M	A S P Q A A G A S A
RK31_Streptomyc	T L T A P G A A V N	T I Q T W L P G A P	V A E A G Y S L P A	G Y G M I Q G T S M	A S P Q A A G A S A
PAM3C_Streptomyc	T L T A P G A A V N	T I Q T W L P G A P	V A E A G Y S L P A	G Y G M I Q G T S M	A S P Q A A G A S A
HNS054_Streptom	T L T A P G A A V N	T I Q T W L P G A P	V A E A G Y S L P A	G Y G M I Q G T S M	A S P Q A A G A S A

	610	620	630	640	650
KN23_Streptomyc	L L L S A A K Q Q R	I D L T P A T L R T	A L T S T A E H I K	G V Q A Y E E G A G	L I D V V D A W K A
JCM_4860_Strept	L L L S A A K Q Q R	I D L T P A T L R T	A L T S T A E H I K	G V Q A Y E E G A G	L I D V V D A W K A
GB4-14_Streptom	L L L S A A K Q Q R	I D L T P A T L R T	A L T S T A E H I K	G V Q A Y E E G A G	L I D V V D A W K A
mutant_SA-27_St	L L L S A A K Q Q R	I D L T P A T L R T	A L T S T A E H I K	G V Q V Y E E G A G	L I D V V D A W K A
ZS0098_Streptom	L L L S A A K Q Q R	I D L T P A T L R T	A L T S T A R H I K	G V Q A Y E E G A G	L I D V V D A W K A
BJ20_Streptomyc	L L L S A A K Q Q R	I D L T P A T L R T	A L T S T A R H I K	G V Q A Y E E G A G	L I D V V D A W K A
RK31_Streptomyc	L L L S A A K Q Q R	I D L T P A T L R T	A L T S T A R H I K	G V Q A Y E E G A G	L I D V V D A W K A
PAM3C_Streptomyc	L L L S A A K Q Q R	I D L T P A T L R T	A L T S T A R H I K	G V Q A Y E E G A G	L I D V V D A W K A
HNS054_Streptom	L L L S A A K Q Q R	I D L T P A T L R T	A L T S T A R H I K	G V Q A Y E E G A G	L I D V V D A W K A

	660	670	680	690	700
KN23_Streptomyc	I R K G A T A H E Y	T V K A P V D T A I	D Q F L K T P G H G	T G L Y D R E G G L	K A G Q K K T Y D I
JCM_4860_Strept	I R K G A T A H E Y	T V K A P V D T A I	D Q F L K T P G H G	T G L Y D R E G G L	K A G Q K K T Y D I
GB4-14_Streptom	I R K G A T A H E Y	T V K A P V D T A I	D Q F L K T P G H G	T G L Y D R E G G L	K A G Q K K T Y D I
mutant_SA-27_St	I R K G A T A H E Y	T V K A P V D T A I	D Q F L K T P G H G	T G L Y D R E G G L	K A G Q K K T Y D I
ZS0098_Streptom	I R K G A T A H E Y	T V K A P V D T A I	D Q F L K T P G Y G	T G L Y D R E G G L	K A G Q K K T Y D I
BJ20_Streptomyc	I R K G A T A H E Y	T V K A P V D T A I	D Q F L K T P G Y G	T G L Y D R E G G L	K A G Q K K T Y D I
RK31_Streptomyc	I R K G A T A H E Y	T V K A P V D T A I	D Q F L K T P G H G	T G L Y D R E G G L	K A G Q K K T Y D I
PAM3C_Streptomyc	I R K G A T A H E Y	T V K A P V D T A I	D Q F L K T P G H G	T G L Y D R E G G L	K A G Q K K T Y D I
HNS054_Streptom	I R K G A T A H E Y	T V K A P V D T A I	D Q F L K T P G H G	T G L Y D R E G G L	K A G Q K K T Y D I

	710	720	730	740	750
KN23_Streptomyc	T I T R T S G P D	A V R H E I D L A N	N A D R T F R V V G	G D T V S L P I N K	P V T V K V Q A Q P
JCM_4860_Strept	T I T R T S G P D	A V R H E I D L A N	N A D R T F R V V G	G D T V S L P I N K	P V T V K V Q A Q P
GB4-14_Streptom	T I T R T T G P D	A V R H E I D L A N	N A D R T F R V V G	G D T V S L P I N K	P V T V K V Q A Q P
mutant_SA-27_St	T I T R T S G P D	A V R H E I D L A N	N A D R T F R V V G	G D T V S L P I N K	P V T V K V Q A Q P
ZS0098_Streptom	T I T R T S G P D	A V R H E I D L A N	N A D R A F R V V G	G S K V S L P I N K	P V T V K V Q A Q S

BJ20_Streptomyc	T	I	T	R	T	S	G	P	D	R	A	V	R	H	E	L	D	L	A	N	N	A	D	R	A	F	R	V	V	G	G	S	K	V	S	L	P	L	N	K	P	V	T	V	K	V	Q	A	Q	S
RK31_Streptomyc	T	I	T	R	T	S	G	P	D	R	A	V	R	H	E	L	D	L	A	N	N	A	D	R	A	F	R	V	V	G	G	S	K	V	S	L	P	L	N	K	P	V	T	V	K	V	Q	A	Q	S
PAM3C_Streptomyc	T	I	T	R	T	S	G	P	D	R	A	V	R	H	E	L	D	L	A	N	N	A	D	R	A	F	R	V	V	G	G	S	K	V	S	L	P	L	N	K	P	V	T	V	K	V	Q	A	Q	S
HNS054_Streptomyc	T	I	T	R	T	S	G	P	D	R	A	V	R	H	E	L	D	L	A	N	N	A	D	R	A	F	R	V	V	G	G	S	K	V	S	L	P	L	N	K	P	V	T	V	K	V	Q	A	Q	S

										760											770																		780																			790																				800																			
KN23_Streptomyc	R	S	A	G	I	K	S	A	I	L	E	V	D	D	E	R	T	E	G	V	D	R	Q	I	L	T	T	V	V	V	S	T	P	L	K	Y	T	Y	S	A	K	G	T	A	Q	R	N	S	T	T																																															
JCM_4860_Strept	R	S	A	G	I	K	S	A	I	L	E	V	D	D	E	R	T	E	G	V	D	R	Q	I	L	T	T	V	V	V	S	T	P	L	K	Y	T	Y	S	A	K	G	T	A	Q	R	N	S	T	T																																															
GB4-14_Streptom	R	S	A	G	I	K	S	A	I	L	E	V	D	D	E	R	T	E	G	V	D	R	Q	I	L	T	T	V	V	V	S	T	P	L	K	Y	T	Y	S	A	K	G	T	A	Q	R	N	S	T	T																																															
mutant_SA-27_St	R	S	A	G	I	K	S	A	I	L	E	V	D	D	E	R	T	E	G	V	D	R	Q	I	L	T	T	V	V	V	S	T	P	L	K	Y	T	Y	S	A	K	G	T	A	Q	R	N	S	T	T																																															
ZS0098_Streptom	R	T	A	G	I	K	S	A	I	L	E	V	D	D	E	R	T	E	G	V	D	R	Q	I	L	T	T	V	V	V	S	T	P	L	K	Y	T	Y	S	A	K	G	T	A	Q	R	N	S	T	T																																															
BJ20_Streptomyc	R	T	A	G	I	K	S	A	I	L	E	V	D	D	E	R	T	E	G	V	D	R	Q	I	L	T	T	V	V	V	S	T	P	L	K	Y	T	Y	S	A	K	G	T	A	Q	R	N	S	T	T																																															
RK31_Streptomyc	R	T	A	G	I	K	S	A	I	L	E	V	D	D	E	R	T	E	G	V	D	R	Q	I	L	T	T	V	V	V	S	T	P	L	K	Y	T	Y	S	A	R	G	T	A	Q	R	N	S	T	T																																															
PAM3C_Streptomyc	R	T	A	G	I	K	S	A	I	L	E	V	D	D	E	R	T	E	G	V	D	R	Q	I	L	T	T	V	V	V	S	T	P	L	K	Y	T	Y	S	A	R	G	T	A	Q	R	N	S	T	T																																															
HNS054_Streptomyc	R	T	A	G	I	K	S	A	I	L	E	V	D	D	E	R	T	E	G	V	D	R	Q	I	L	T	T	V	V	V	S	T	P	L	K	Y	T	Y	S	A	R	G	T	A	Q	R	N	S	T	T																																															

										810											820																		830																			840																				850																			
KN23_Streptomyc	S	Y	F	V	T	V	P	E	G	A	K	T	L	E	V	A	M	S	G	L	K	A	T	S	Q	T	R	F	I	S	I	H	P	Y	G	V	P	S	D	P	T	S	T	V	N	C	Y	P	N	Y																																															
JCM_4860_Strept	S	Y	F	V	T	V	P	E	G	A	K	T	L	E	V	A	M	S	G	L	K	A	T	S	Q	T	R	F	I	S	I	H	P	Y	G	V	P	S	D	P	T	S	T	V	N	C	Y	P	N	Y																																															
GB4-14_Streptom	S	Y	F	V	T	V	P	E	G	A	K	T	L	E	V	A	M	S	G	L	K	A	T	S	Q	T	R	F	I	S	I	H	P	Y	G	V	P	S	D	P	T	S	T	V	N	C	Y	P	N	Y																																															
mutant_SA-27_St	S	Y	F	V	T	V	P	E	G	A	K	T	L	E	V	A	M	S	G	L	K	A	T	S	Q	T	R	F	I	S	I	H	P	Y	G	V	P	S	D	P	T	S	T	V	N	C	Y	P	N	Y																																															
ZS0098_Streptom	S	Y	F	V	T	V	P	E	G	A	K	T	L	E	V	A	M	S	G	L	K	A	T	S	Q	T	R	F	I	S	I	H	P	Y	G	V	P	A	D	P	T	S	T	V	N	C	Y	P	N	Y																																															
BJ20_Streptomyc	S	Y	F	V	T	V	P	E	G	A	K	T	L	E	V	A	M	S	G	L	K	A	T	S	Q	T	R	F	I	S	I	H	P	Y	G	V	P	A	D	P	T	S	T	V	N	C	Y	P	N	Y																																															
RK31_Streptomyc	S	Y	F	V	T	V	P	E	G	A	K	T	L	E	V	A	M	S	G	L	K	A	T	S	Q	T	R	F	I	S	I	H	P	Y	G	V	P	A	D	P	T	S	T	V	N	C	Y	P	N	Y																																															
PAM3C_Streptomyc	S	Y	F	V	T	V	P	E	G	A	K	T	L	E	V	A	M	S	G	L	K	A	T	S	Q	T	R	F	I	S	I	H	P	Y	G	V	P	A	D	P	T	S	T	V	N	C	Y	P	N	Y																																															
HNS054_Streptomyc	S	Y	F	V	T	V	P	E	G	A	K	T	L	E	V	A	M	S	G	L	K	A	T	S	Q	T	R	F	I	S	I	H	P	Y	G	V	P	A	D	P	T	S	T	V	N	C	Y	P	N	Y																																															

										860											870																		880																			890																				900																			
KN23_Streptomyc	S	N	P	A	N	T	C	R	P	D	V	R	S	Y	A	D	F	Q	P	G	V	W	E	I	E	V	E	A	R	R	T	S	P	L	L	D	N	P	Y	T	L	D	V	A	A	L	G	A	A	F																																															
JCM_4860_Strept	S	N	P	A	N	T	C	R	P	D	V	R	S	Y	A	D	F	Q	P	G	V	W	E	I	E	V	E	A	R	R	T	S	P	L	L	D	N	P	Y	T	L	D	V	A	A	L	G	A	A	F																																															
GB4-14_Streptom	S	N	P	A	N	T	C	R	P	D	V	R	S	Y	A	D	F	Q	P	G	V	W	E	I	E	V	E	A	R	R	T	S	P	L	L	D	N	P	Y	T	L	D	V	A	A	L	G	A	A	F																																															
mutant_SA-27_St	S	N	P	A	N	T	C	R	P	D	V	R	S	Y	A	D	F	Q	P	G	V	W	E	I	E	V	E	A	R	R	T	S	P	L	L	D	N	P	Y	T	L	D	V	A	A	L	G	A	A	F																																															
ZS0098_Streptom	S	N	P	A	N	T	C	R	P	D	V	R	S	Y	A	N	F	Q	P	G	V	W	E	I	E	V	E	S	R	R	T	S	P	L	L	D	N	P	Y	K	L	D	V	A	V	L	G	A	A	F																																															
BJ20_Streptomyc	S	N	P	A	N	T	C	R	P	D	V	R	S	Y	A	N	F	Q	P	G	V	W	E	I	E	V	E	S	R	R	T	S	P	L	L	D	N	P	Y	K	L	D	V	A	V	L	G	A	A	F																																															
RK31_Streptomyc	S	N	P	A	N	T	C	R	P	D	V	R	S	Y	A	N	F	Q	P	G	V	W	E	I	E	V	E	S	R	R	T	S	P	L	L	D	N	P	Y	K	L	D	V	A	V	L	G	A	A	F																																															
PAM3C_Streptomyc	S	N	P	A	N	T	C	R	P	D	V	R	S	Y	A	N	F	Q	P	G	V	W	E	I	E	V	E	S	R	R	T	S	P	L	L	D	N	P	Y	K	L	D	V	A	V	L	G	A	A	F																																															
HNS054_Streptomyc	S	N	P	A	N	T	C	R	P	D	V	R	S	Y	A	N	F	Q	P	G	V	W	E	I	E	V	E	S	R	R	T	S	P	L	L	D	N	P	Y	K	L	D	V	A	V	L	G	A	A	F																																															

										910											920																		930																			940																				950																			
KN23_Streptomyc	D	P	E	T	V	T	V	P	E	A	K	V	G	T	P	A	G	V	D	W	T	V	T	N	E	A	A	A	I	D	G	R	L	V	G	G	P	L	G	S	S	K	T	A	R	P	S	I	G	T																																															
JCM_4860_Strept	D	P	E	T	V	T	V	P	E	A	K	V	G	T	P	A	G	V	D	W	T	V	T	N	E	A	A	A	I	D	G	R	L	V	G	G	P	L	G	S	S	K	T	A	R	P	S	I	G	T																																															
GB4-14_Streptom	D	P	E	T	V	T	V	P	E	A	K	V	G	T	P	A	G	V	D	W	T	V	T	N	E	A	A	A	I	D	G	R	L	V	G	G	P	L	G	S	S	K	T	A	R	P	S	I	G	T																																															
mutant_SA-27_St	D	P	E	T	V	T	V	P	E	A	K	V	G	T	P	A	G	V	D	W	T	V	T	N	E	A	A	A	I	D	G	R	L	V	G	G	P	L	G	S	S	K	T	A	R	P	S	I	G	T																																															
ZS0098_Streptom	D	P	E	T	V	T	V	P	E	A	K	V	G	T	P	A	S	V	E	W	T	V	T	N	E	A	A	A	I	D	G	K	L	V	G	G	P	L	G	S	S	K	T	A	R	P	S	I	G	T																																															
BJ20_Streptomyc	D	P	E	T	V	T	V	P	E	A	E	V	G	T	P	A	S	V	E	W	T	V	T	N	E	A	A	A	I	D	G	K	L	V	G	G	P	L	G	S	S	K	T	A	R	P	S	I	G	T																																															

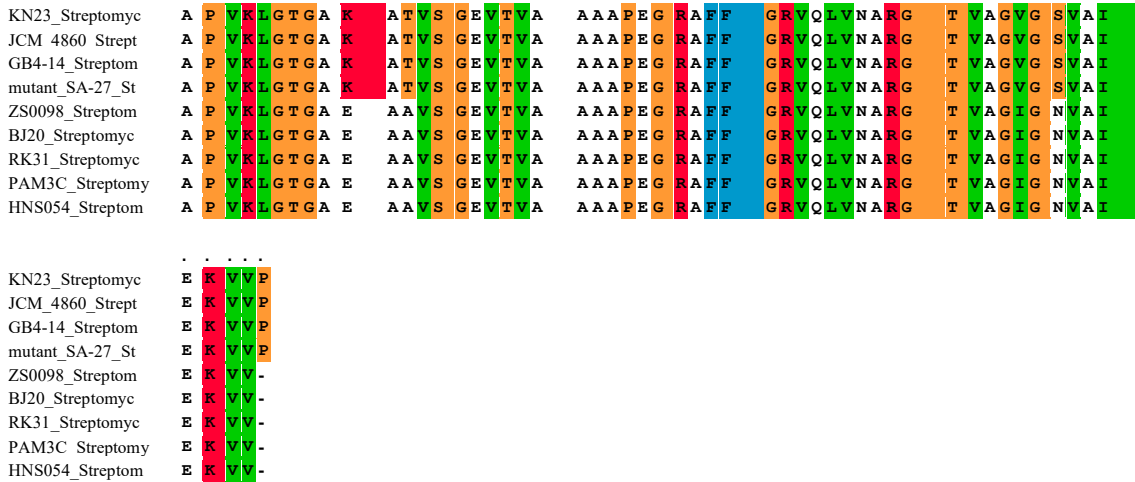
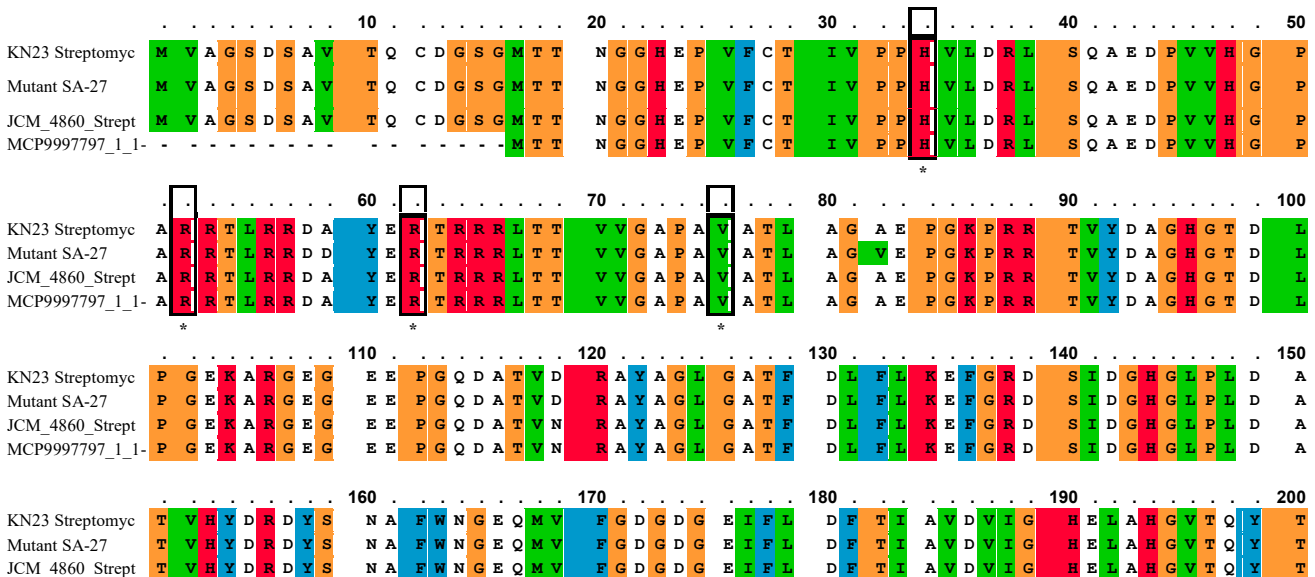


Fig. 1: Multiple sequence alignment of the experimentally determined amino acids for *serine protease (SerPr)* from the *streptomyces* family. Amino acid sequence alignment was performed by PSI-BLAST pre-profile processing (Homology-extended alignment) available from the PRALINE online resource portal (<http://www.ibi.vu.nl/programs/pralinewww/>). Active site residues across the *metalloprotease (SertPr)* are marked with black color “*”.

The multiple sequence alignment analysis revealed the presence of four consensus regions in the *metalloprotease (MetPr)* sequences. Among them, the sequence of *S. werraensis* KN23 and mutant *S. werraensis* SA27 exhibited the highest degree of similarity to the *metalloprotease (MetPr)* sequence of *S. werraensis* JCM 4860, indicating their close relationship within the *Streptomyces* genus. Notably, investigations focused on the active site of the *metalloprotease (MetPr)* enzymes from *S. werraensis* KN23 and mutant *S. werraensis* SA27, which revealed the presence of eight amino acid substitutions HIS34, ARG52, ARG62, VAL282, VAL76, THR326, HIS202, and GLN332 at specific positions, as depicted in Figure 2.

G, P, S, T, H, K, R, F, W, Y, I, L, M, V



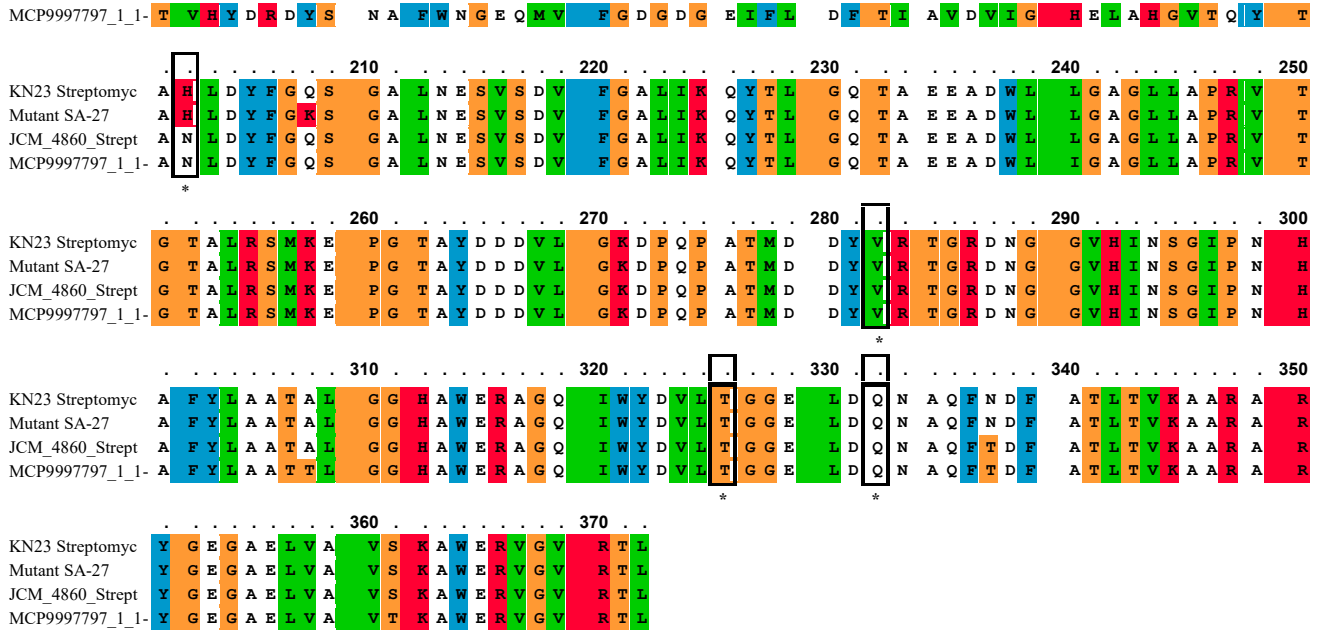


Fig. 2: Multiple sequence alignment of the experimentally determined amino acids for metalloprotease (*MetPr*) from the *streptomyces* family. Amino acid sequence alignment was performed by PSI-BLAST pre-profile processing (Homology-extended alignment) available from the PRALINE online resource portal (<http://www.ibi.vu.nl/programs/pralinewww/>). Active site residues across the metalloprotease (*MetPr*) are marked with black color “*”.

In a related studies of Gupta *et al.* (2017) Performed comparative analysis of the *ker* enzyme, found by experimentation, with other *subtilisin* enzymes from the *Bacillus* family using multiple sequence alignment. The PDB codes for the remaining enzymes are provided. Nahar *et al.* (2016) documented Matrix comparison of the mature (274 aa) protein from *B. licheniformis* strain MZK-05 with other strains' *KerA* and *Subtilisin* Carlsberg proteins, which are closely related. The enzyme *Subtilisin* Carlsberg often abbreviated as SC. Several differences were found in the *KerA* protein from *B. licheniformis* MZK-05. These include the substitution of Tyr26 for Phe26 and the substitution of Asn86 and Ser211 for Ser86 and Asn211, respectively. The pro-peptide sequence alignment of keratinases from various sources was reported by Peng *et al.* (2021). Using pro-peptide multiple sequence alignment, eight sequences Recombinant keratinase KerZ1 yielded keratinases that were substantially expressed and active, with a range of 16% to 66%. Rahimnahal *et al.* (2023) have a protein sequence alignment study of many closely related sequences with the keratinase KRLr1 from *Bacillus licheniformis*. The *KerS* gene's amino acid sequence was compared to *Bacillus cereus* group S8 family peptidase sequences found in GenBank. This finding was published by Almahasheer *et al.* (2022). A research examining the amino acid sequences of *B. cereus* identified a total of 19 amino acid alterations, according to Abdel-Naby *et al.* (2020). The alterations resulted in a significant improvement of around 31.17% in the protease compared to the wild type. Specifically, nine of the substitutions led to an increase in the enzyme's catalytic effectiveness (Abd El-Aziz *et al.*, 2023b), Using multiple sequence alignment, the experimentally determined amino acids for the *Pichia* family's metalloprotease (*MetPr*) were brought together. To identify the *endo-polygalacturonase* PGI enzyme belonging to the *Rhodotorula* family, iterative sequence alignment of empirically determined amino acids was used by Abd El Aziz *et al.* (2023c).

3.3. Cluster analysis (phylogenetic tree) of *Streptomyces werraensis* serine protease (*SerPr*) and metalloprotease (*MetPr*) sequence

This step involved conducting a phylogenetic analysis to position *serine protease* (*SerPr*) and *metalloprotease* (*MetPr*) proteins within the family of known *serine protease* (*SerPr*) and

metalloprotease (*MetPr*) proteins. The thirteen *serine protease* (*SerPr*) and *metalloprotease* (*MetPr*) proteins chosen from the curated UniProt protein library to represent different strains were then inserted into a phylogenetic tree using MEGAX software. The dataset included *SerPr* and *MetPr* proteins from *S. werraensis* JCM 4860, *S. werraensis* KN23, and mutant *S. werraensis* SA27. The results showed that all *Streptomyces* genotypes of *SerPr* and *MetPr* proteins were divided into several main cluster proteins. The results indicated that *S. werraensis* JCM 4860, *S. werraensis* KN23, and mutant *S. werraensis* SA27 were closely related to the *SerPr* and *MetPr* of *Streptomyces* in the same cluster, as illustrated in Figs. 3a and 3b.

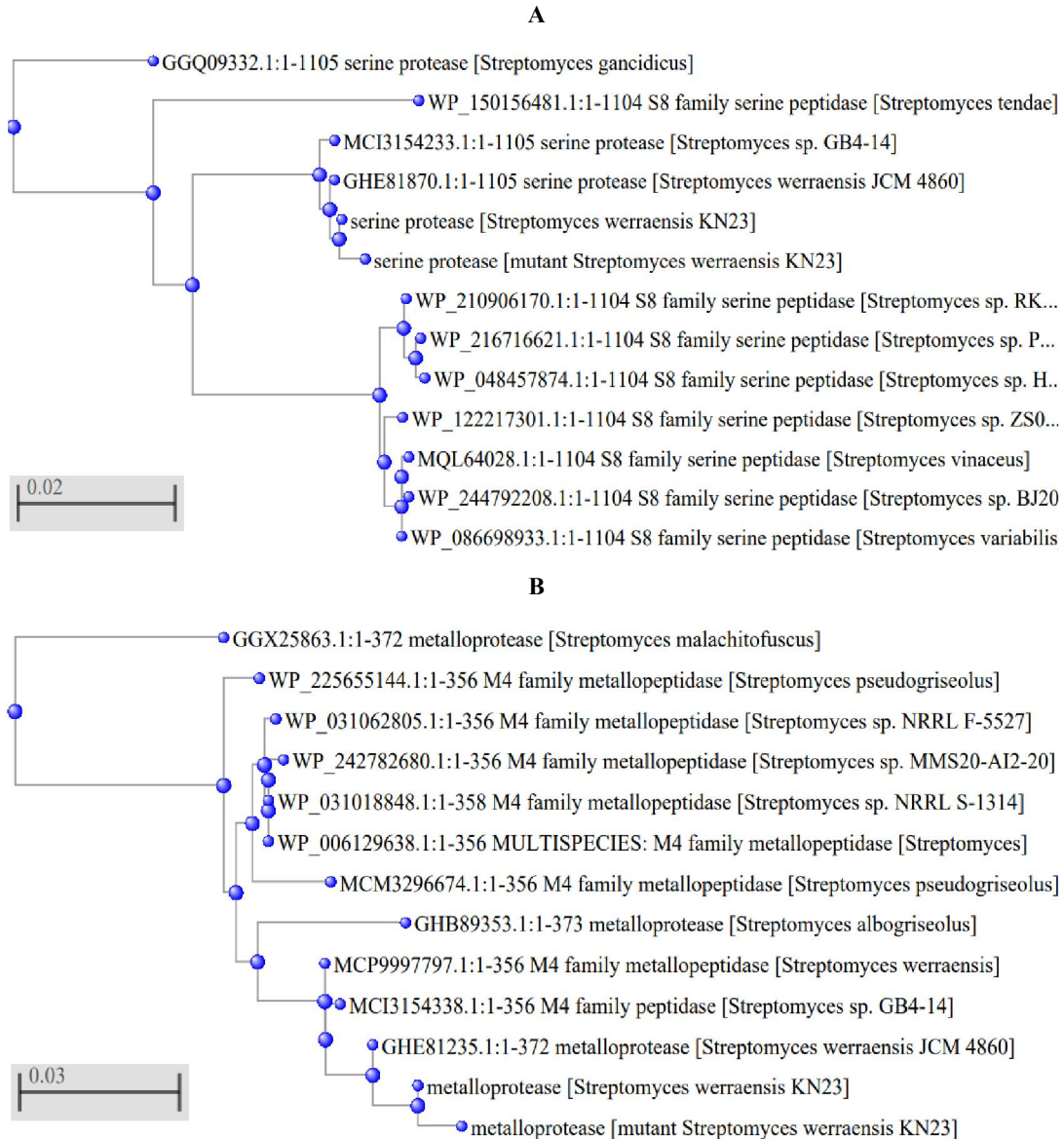


Fig. 3: Phylogenetic tree of **A**; thirteen strains *streptomyces SerPr* protein sequences, **B**; thirteen streptomyces *MetPr* protein sequences were constructed using the neighbour-joining method (MEGAX) software.

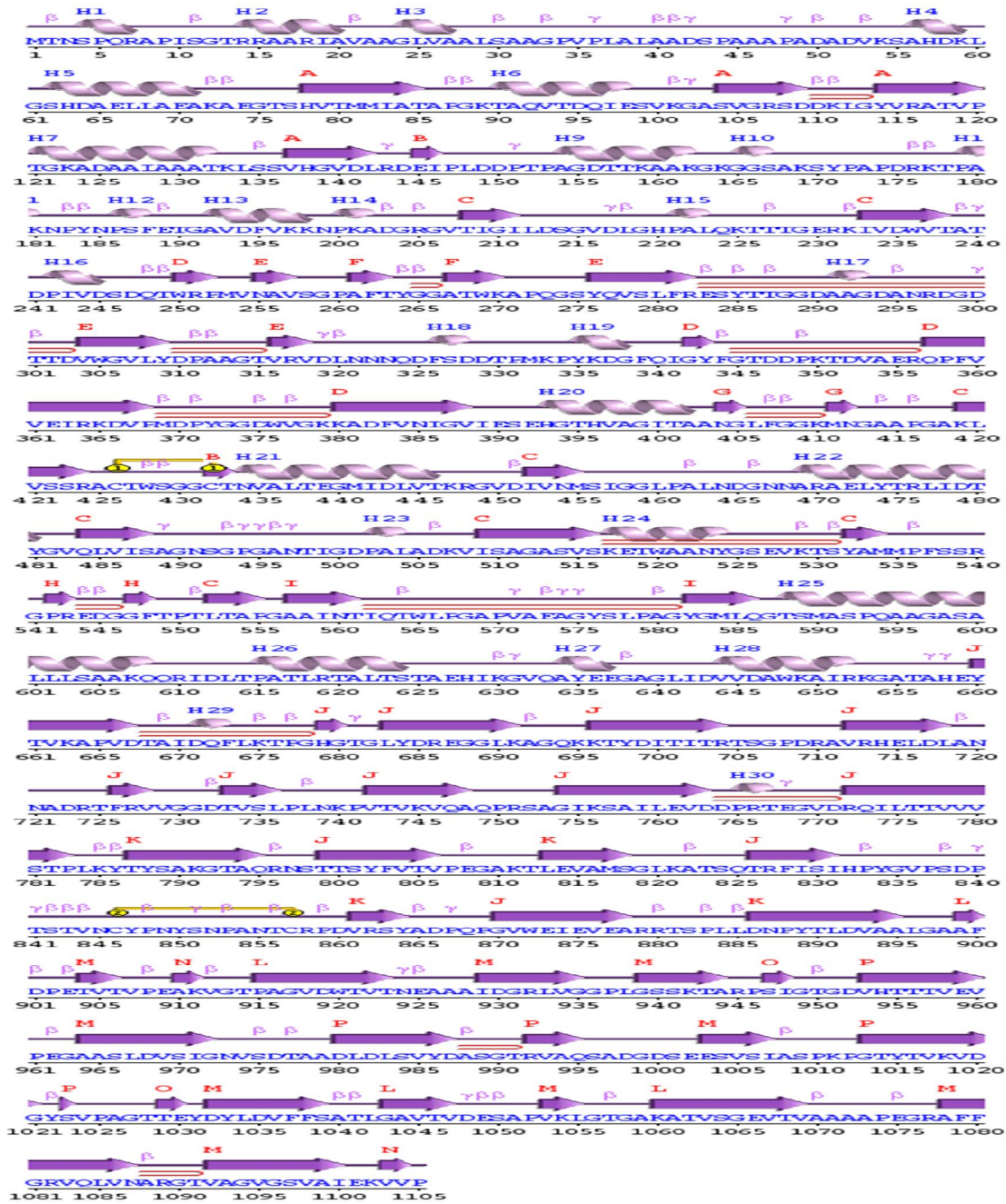
Based on a phylogenetic tree study published by, *Bacillus licheniformis* keratinase, a member of the *serine peptidase/subtilisin*-like S8 family, showed the greatest degree of similarity to KRLr1 and associated amino acid sequences in related research (Rahimnahal *et al.*, 2023). The unrooted neighbor-joining (NJ) tree was built using protein sequence alignments that had a high degree of similarity. In a related study of (Abd El-Aziz *et al.*, 2023b), reported eight yeast strains *Pichia MetPr* protein sequences were utilized to create the phylogenetic tree using the neighbor-joining approach (MEGAX) software. Abd El-Aziz *et al.* (2023c), reported based on the *Rhodotorula endo-PGI* protein sequences and the ten strains phylogenetic tree, the MEGA X program used a neighbor-joining approach.

3.4. Secondary structure prediction of *serine protease (SerPr)* and *metalloprotease (MetPr)* protein

Use the *S. werraensis* JCM 4860, *S. werraensis* KN23, and mutant *S. werraensis* SA27 as templates to align the *SerPr* and *MetPr* proteins and predict their secondary structures. The experiments were conducted using the PDBsum service. According to the *SerPr* model characterization in the PDBsum, the predicted *SerPr* enzyme for *S. werraensis* KN23 has the following topology and secondary structure: 68 strands, 30 helices, 16 helix-helix interactions, 114 beta turns, and 35 gamma turns. The model also includes 1 beta alpha beta unit, 14 beta hairpins, 19 beta bulges, and 68 sheets. In contrast, mutant *S. werraensis* SA27 has 67 strands, 25 helices, 14 helix-helix interactions, 113 beta turns, and 39 gamma turns, as seen in Figure 4a and 4b; there are also 1 beta alpha beta unit and 16 sheets. According to the *MetPr* model characterization in the PDBsum, the *MetPr* enzyme in *S. werraensis* KN23 is expected to have the following topology and secondary structure: two sheets, three beta hairpins, three beta bulges, seven strands, fourteen helices, seventeen helix-helix interactions, thirty-five beta turns, and seven gamma turns. In addition, mutant *S. werraensis* SA27 has two sheets, three beta hairpins, three beta bulges, seven strands, twelve helices, sixteen helix-helix interactions, forty beta turns, and five gamma turns, as seen in Figure 5a and 5b.

Similarly, in a study of Rahimnahal *et al.* (2023) the KRLr1 is composed of a secondary structure with an α -helix making up 25% of its total mass and a β -sheet accounting for 27%, as shown by the data collected from the NetSurfP-2.0 website. Predicted KRLr1 active site cleft amino acids are close to the *Bacillus subtilis subtilisin E* structure. Asn294, Ser297, His75, Asp136, Asn138, His140, Leu172, Ser175, Ser177, Ser232, Ala279, Thr292, Ser179, and KRLr1 are the amino acids shown by the orange sticks. Using the superimposition command in Chimera V13.1, the modeled structure of KRLr1 was compared with three structures that are very similar to *Bacillus subtilis subtilisin*. (Abd El-Aziz *et al.*, 2023b) the predicted *MetPr* enzyme in *Pichia kudriavzevii* strain 129 has a secondary structure that includes 57 β sheets and 18 α -helices. The enzyme in the YK46 strain of *Pichia kudriavzevii* has a secondary structure that includes 55 β sheets and 18 α -helices. (Abd El-Aziz *et al.*, 2023c) we looked at the secondary structure and topology of the projected *endo-PGI* enzyme. It was found that *Rhodotorula mucilaginosa endo-PGI-PY18* has twenty-two α -helices and four β sheets. The *endo-PGI-E54* strain of *Rhodotorula mucilaginosa* has twenty-one α -helices and three β sheets. The C6P46_003867 *Rhodo-PGI* strain KR endo-PGI putative template protein has 21 α -helices (H) and 3 β sheets (E).

A



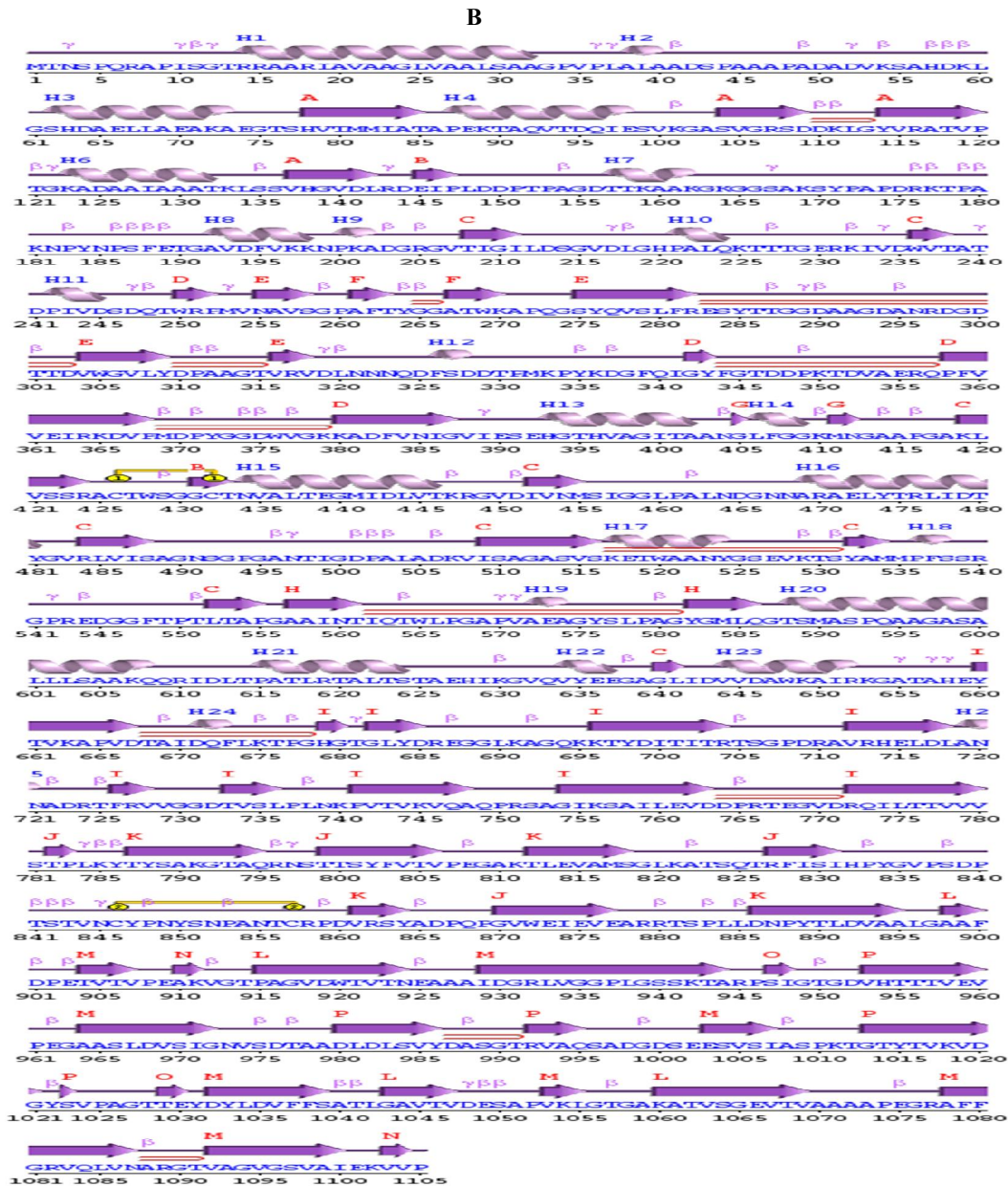


Fig. 4: Predicted secondary structure of *SerPr* protein: A, secondary structure of *S. werraensis* KN23; B; secondary structure of mutant *S. werraensis* SA27.

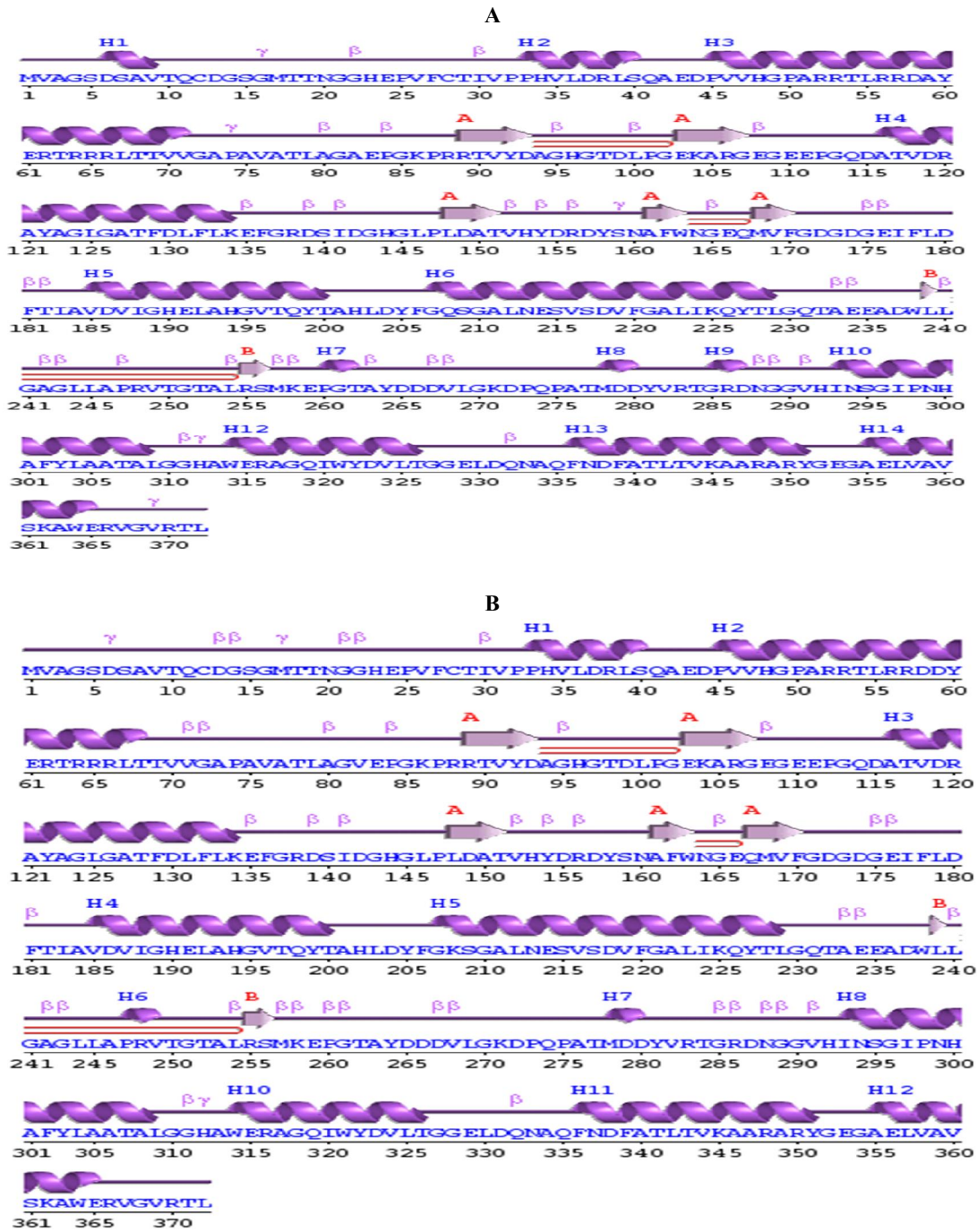


Fig. 5: Predicted secondary structure of *MetPr* protein: A, secondary structure of *S. werraensis* KN23; B, secondary structure of mutant *S. werraensis* SA27.

3.5. Homology modelling and validation of *serine protease (SerPr)* and *metalloprotease (MetPr)*

When it comes to modeling protein sequences without structural knowledge, it is necessary to apply program for predicting the three-dimensional structure of proteins. Understanding how proteins interact with ligands or other molecules improves our understanding of the connection between protein sequence, dynamics, structure, and function (Yang and Yang, 2015). We modeled the *serine protease* homologously to (*SerPr*) and *metalloprotease (MetPr)* proteins from template *S. werraensis* strain JCM 4860, *S. werraensis* KN2 and mutant *S. werraensis* SA27, I-TASSER, ROBETTA and Phyre2 were used (Kathwate 2020; Heo *et al.*, 2013). As a last step in the experimental process, the ROBETTA server—an interactive platform for template-based predictions of protein structure and function—was used to choose the best model. To simulate iterative structural assembly and numerous threading alignments, ROBETTA creates full-length atomic models from the most important template. Then, it refines the structure at the atomic level, beginning with the amino acid sequence of the target protein (Zhang 2008; Kulkarni and devarumath 2014). Using ROBETTA, a total of five models were created. After evaluating each model's potential energy and confidence score (C-score), the best model was chosen for future investigation (Roy *et al.*, 2012; Zheng *et al.*, 2021; Singh and Muthusamy 2013). A C-score was computed by taking into account the parameters produced during structure assembly simulations, the outcome of alignment among threaded structures, and the employed template (Patni *et al.*, 2021; Roy *et al.*, 2012). The typical range for a C-score is between 0 and 1. In this case, there is a direct correlation between the C-score and the quality of the structure. One example is for this round of testing, we used the model with the highest C-score. Increased trust and reliability in a model are indicators of a high C-score (Yang and Yang, 2015).

In our study, using the ROBETTA server, five models were generated for the *serine protease (SerPr)* 1105 residues for both the template strain *S. werraensis* JCM 4860, *S. werraensis* KN23, and mutant *S. werraensis* SA27. Model 2 of the five separate *SerPr* residues models was selected for more research because to its high C-score and low estimate error, as determined by the cluster densities. We chose it because the model for the template has a high C-score of 0.79, which means we have a lot of faith in it template strain *S. werraensis* JCM4860, as shown in Figure 6a. Model 1, which had the greatest C-score and a low estimate error, was chosen for further study. A high C-score implies a high level of confidence in the model, specifically a score of 0.80 for the strain *S. werraensis* KN23, as shown in Figure 6b. Model 4, which mean the greatest C-score and minimal estimate error, was chosen for further study. A high C-score of 0.79 suggests a high level of confidence in the model for the mutant strain *S. werraensis* SA27, as shown in Figure 6c.

Using the ROBETTA server, five models were generated for the *metalloprotease (MetPr)* 372 residues for both the template strain *S. werraensis* JCM 4860, *S. werraensis* KN23, and mutant *S. werraensis* SA27. Based on their cluster density, The C-scores (confidence scores) for the different five models of the *MetPr* residues Model 3, with the highest C-score and low estimation error, was selected for further analysis since a high C-score indicates high confidence in the model of 0.81 for the template strain *S. werraensis* JCM4860, as illustrated in Fig. 7a. Model 5, with the highest C-score and low estimation error, was selected for further analysis since a high C-score indicates high confidence in the model of 0.81 for the strain *S. werraensis* KN23, as illustrated in Fig. 7 b. Model 2, with the highest C-score and low estimation error, was selected for further analysis since a high C-score indicates high confidence in the model of 0.81 for mutant strain *S. werraensis* SA27, as illustrated in Fig. 7c.

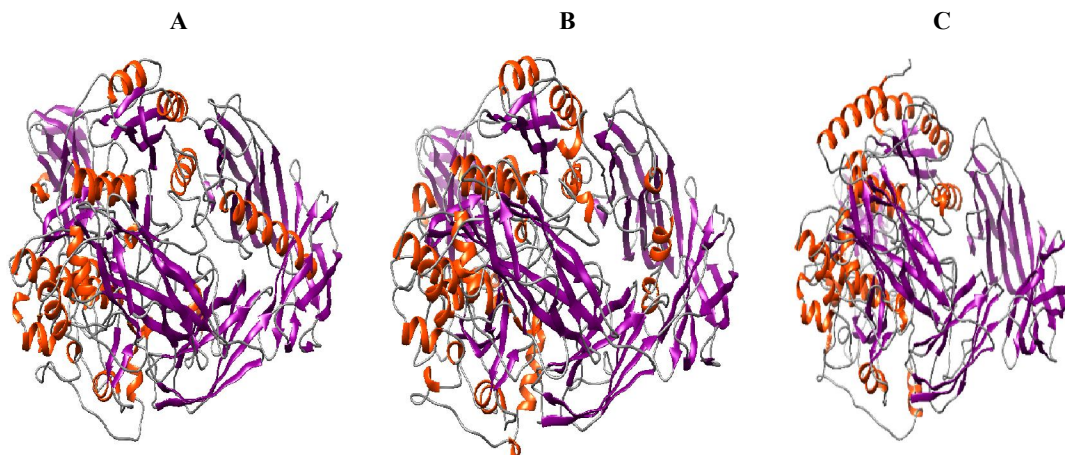


Fig. 6: Modelled 3D structure of *SerPr* protein: A, template *S. werraensis* JCM 4860; B, *S. werraensis* KN23; C, mutant *S. werraensis* SA27.

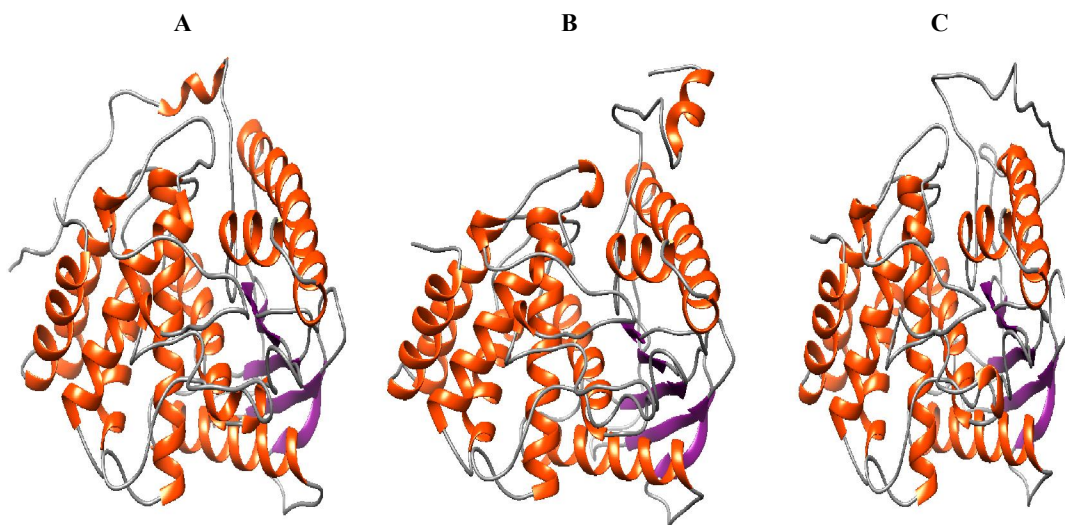


Fig. 7: Modelled 3D structure of *MetPr* protein: A, template *S. werraensis* JCM 4860; B, *S. werraensis* KN23; C, mutant *S. werraensis* SA27.

Next, the generated model was evaluated using general stereochemical parameters by the PROCHECK server. Additionally, the ramachandran plot of the energy-minimised model of *serine protease (SerPr)* and *metalloprotease (MetPr)* structures was generated, which splits the x-axis into four quadrants representing the low-energy region, allowed region, generally allowed region, and disallowed region. Analyzed by PROCHECK, the 3D-modeled template strain *S. werraensis* JCM 4860 *SerPr* protein exhibited 1105 residues, representing 91.08% they contribute to overall quality. In addition, the Ramachandran plot's most favorable regions included 97.8% of these residues. Plus, in the generously authorized areas, 10.0% of residues were detected, in the further permissible areas, 1.2%, and in the banned sections, 1.0%, as shown in Figure 8a. The strain *S. werraensis* KN23 *SerPr* protein, which was created as a 3D model, was examined using PROCHECK. The analysis Results showed that 1105 residues, representing (or 91.39% of the total quality factor), and 85.2% of the residues were in the most favorable areas of the Ramachandran plot. Furthermore, 12.4% of the residues) were located in the further permitted areas, 1.1% in the generously allowed regions, and

1.3% in the banned regions, as seen in Figure 8b. Analyzed by PROCHECK, the mutant strain *S. werraensis* SA27 *SerPr* protein, which was modeled in 3D showed that 1105 residues, representing 91.93% of the total quality factor, were located in the most preferred areas of the Ramachandran plot, accounting for overall quality factor, which made up 87.6% of residues, were found in the further permitted areas, 0.9% in the generously allowed regions, and 1.5% in the banned regions, as seen in Figure 8c.

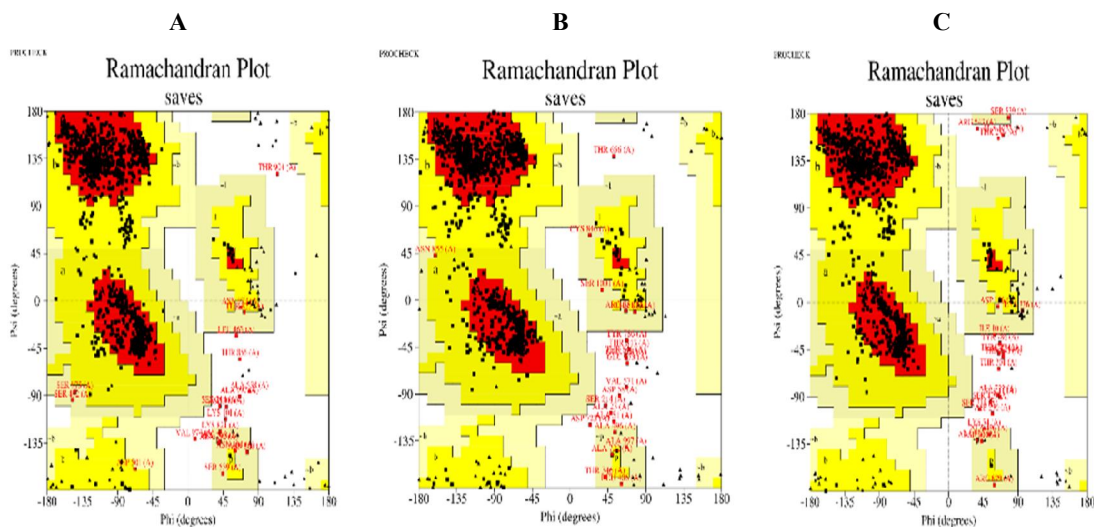


Fig. 8: Ramachandran plot of *SerPr* protein: **A**, template *S. werraensis* JCM 4860; **B**, *S. werraensis* KN23; **C**, mutant *S. werraensis* SA27.

The 3D-modelled template strain *S. werraensis* JCM4860 *MetPr* protein was analysed using PROCHECK, which revealed that 372 residues, accounting for 98.87% of the overall quality factor, and 90.2% of the areas of the Ramachandran plot that were most advantageous have residues. On top of that, 9.4 percent of leftovers were in specifically permitted areas, 0.3 percent in areas that were liberally tolerated, and 0 percent in areas that were prohibited, as illustrated in Fig. 9a. An analysis of the 3D-modeled *S. werraensis* KN23 *MetPr* protein was conducted using PROCHECK. The results showed that out of the total quality factor, which was 99.43%, 372 residues (or 92.8% of the total) were located in the most favorable areas of the Ramachandran plot. The percentage of residues in the extra permitted areas was 7.2%, the percentage in the generously allowed regions was 0%, and the percentage in the banned sections was 0%, as illustrated in Fig. 9b. Through the application of PROCHECK to the 3D-modeled mutant strain *S. werraensis* SA27 *MetPr* protein, it was discovered that 372 residues, or 93.05% of the total quality factor, and 88.6% of residues were in the most beneficial regions of the Ramachandran plot. Also in the permitted zones, 11.1% of residues were detected, while in the generously allowed sections, 0% were discovered and in the forbidden sectors, 0.3% were identified, as illustrated in Fig. 9c.

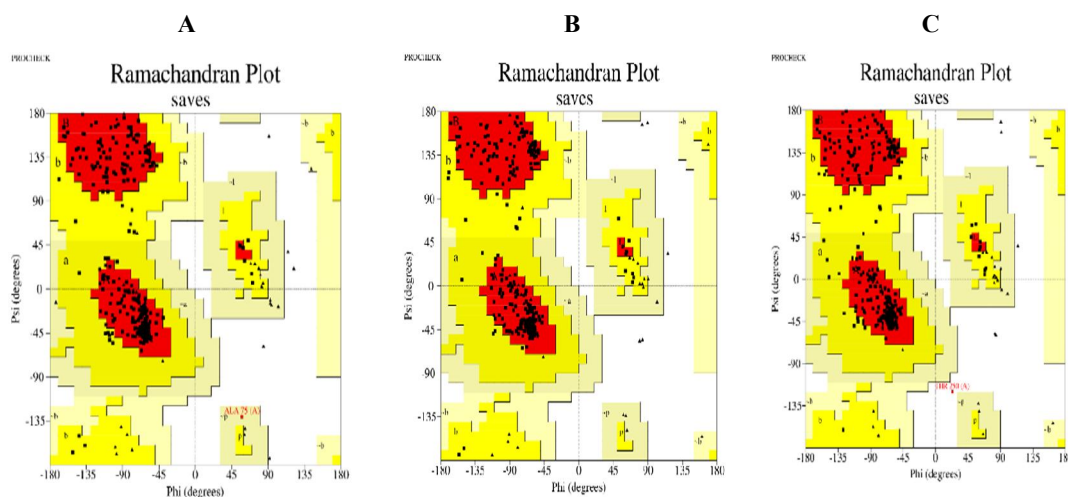


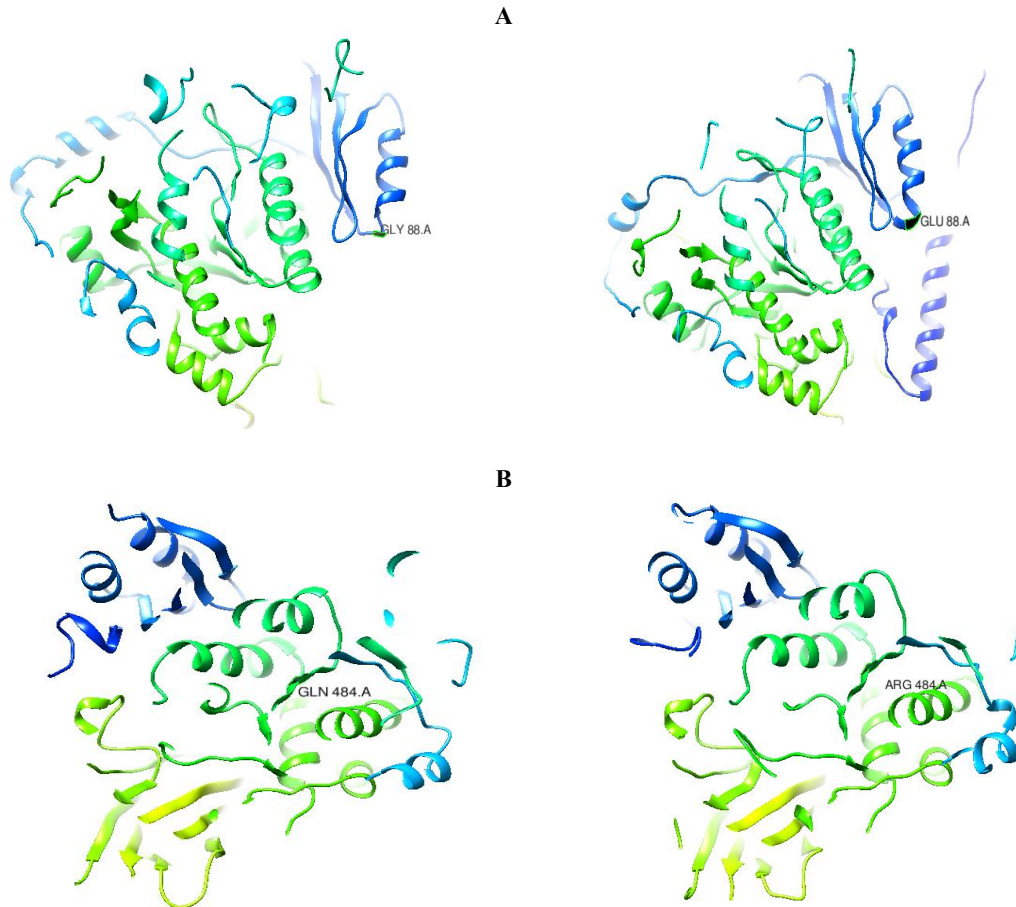
Fig. 9: Ramachandran plot of *MetPr* protein: A, template *S. werraensis* JCM 4860; B, *S. werraensis* KN23; C, mutant *S. werraensis* SA27.

In related studies of Gupta *et al.*, 2017 the RSE163 keratinase *ker* gene from *Bacillus subtilis*, which encodes 447 amino acids employing 1342 base pairs. Ramachandran's plot, which shows 305 residues (84.3%) in the most preferred region, was used to validate the structure3D model. Structure and topology of the keratinase enzyme that has been predicted showed its units, which are twelve alpha helices (H1–H12) and sixteen stranded beta sheets (AE), whereas motifs denoted by the letters beta (β) and gamma (γ) turn with beta hairpin (\odot). Additionally, the mature peptide has, in order, 29, 76, and 274 amino acids. Using the Swiss-Model programme, homology modelling was performed to estimate the keratinase KerZ1 protein structure. Two α -helices and five β -sheets were found in the pro-peptide part of the protein, according to the analysis (Waterhouse *et al.*, 2018). It is widely acknowledged that α helices and β sheets play a critical role in determining the structure and function of proteins (Marcos *et al.*, 2018). Hence, we performed successive removals of these structural elements to examine the significance of the pro-peptide in the production of the fully developed enzyme. Also Patni *et al.* (2021), performed tertiary structure modelling: the protein's tertiary structure was predicted by I-TASSER. For the additional trial, the C score of -0.68 with a TM-score of 0.63 ± 0.14 and an RMSD of $8.4 \pm 4.5 \text{ \AA}$ was selected. A viable topological model is suggested by a TM-score larger than 0.5, while random similarity is implied by a TM-score less than 0.17. Also, structure validation was carried out: The SAVES v5.0 server was used to validate the refined I-TASSER structure obtained via the galaxy refine tool. The Ramachandran plot was assessed using PROCHECK. According to the Ramachandran plot, 82.7% of the protein residues were located in the most preferred area. Additionally, just 2.7% of the residues were detected in the banned region, while 13.0% and 1.7% of the residues were found in the allowed and generously allowed sectors, respectively. (Nahar *et al.*, 2016) to replicate the three-dimensional structures of the PDB templates 4gi3.1.A, 1yu6.1.A, and 1c3l.1.A, which had sequence identities of 98.54%, 97.81%, and 98.18% with our protein sequence, we conducted simulations, the three-dimensional models of *KerA Bacillus licheniformis* MZK-05/MZK05 were constructed using ProMod Version 3.70. Models 01, 02, and 03 were the names of the models that simulated 4gi3.1.A, 1yu6.1.A, and 1c3l.1.A, respectively. Models 01, 02, and 03 were projected to have QMEAN scores of 0.60, 0.11, and -0.08 , respectively, and were predicted to have no ligand binding sites, $1 \times \text{Ca}^{2+}$, and $2 \times \text{Ca}^{2+}$. According to Rahimnahl *et al.* (2023) Modeller V.9 was used to model the published *Bacillus subtilis* keratinase KRLr1 PDB, using 3WHI PDB as a template structure. The ModRefine server was used to refine the KRLr1 PDB structure, and the PROSA and PROCHECK servers were used to survey the modelled KRLr1 for validation. The projected values for the ERRAT quality factors and Verify-3D scores were 93.06% and 58, respectively. The amino acids KRLr1 are well-positioned at the angles phi (ϕ) and psi (ψ), according to the Ramachandran graph data, which show that 90% of the amino acids were in the favoured, 8% in the allowed, and 2% in the outlier regions following refinement. It is evident from the

validation results that KRLr1 has been accurately modelled. Almahasheer *et al.* (2022) provided Ramachandran plot demonstrating 91.98% of the allowed region and 1.43% of the disallowed region, indicating model validation of the keratinase 3D structure. The amino acids A324 SER, A46 GLN, A160 VAL, A137 ASP, and A114 PRO are not in the favored region. Abd El-Aziz *et al.* (2023b) to determine the *metalloprotease* protein's three-dimensional structure, the I-TASSER tool was used. To confirm the structural accuracy, Ramachandran's plot was used. The results showed that 93% of the 557 residues were in the optimal position for the *MetPr* proteins of the *Pichia kudriavzevii* strain 129 template and 97.26% for the *Pichia kudriavzevii* YK46 template (Abd El-Aziz *et al.*, 2023c), the I-TASSER method was used to determine the three-dimensional structure of the *endo-PGI* enzyme, which is composed of 485 amino acid residues. Verification of the model's correctness was achieved by examining its conformation using Ramachandran's plot. The analysis showed that the template *Rhodotorula mucilaginosa* KR, strain *Rhodotorula mucilaginosa* PY18 and mutant *Rhodotorula mucilaginosa* E54 had 87.71%, 85.56%, and 91.57% of their residues located in the most favorable location, respectively.

3.6. Serine protease (*SerPr*) and metalloprotease (*MetPr*) protein sequence analysis

Comparison of *SerPr* protein sequence of the *S. werraensis* KN23, mutant *S. werraensis* SA27 strains, showed three amino acids substitutions of GLY88GLU, GLN484ARG and ALA634VAL in *S. werraensis* KN23, mutant *S. werraensis* SA27 that led to an improvement of the catalytic efficiency of keratinase by mutant strain compared with the wild type, as described in figure10. Comparison of *MetPr* protein sequence of the *S. werraensis* KN23, mutant *S. werraensis* SA27 strains, showed two amino acids substitutions of ALA82VAL and GLN208LYS in *S. werraensis* KN23, mutant *S. werraensis* SA27 that caused the mutant strain to outperform the wild type in terms of keratinase catalytic efficiency, as described in fig 11.



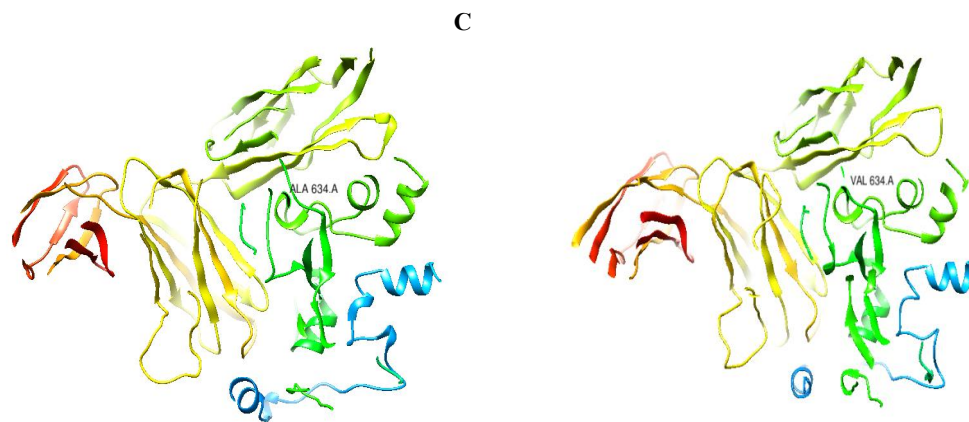


Fig. 10: Amino acid substitution of *SerPr* of: **A;** GLY88GLU, **B;** GLN484ARG and **C;** ALA634VAL in black color, of wild type *S. werraensis* KN23 and mutant *S. werraensis* SA27.

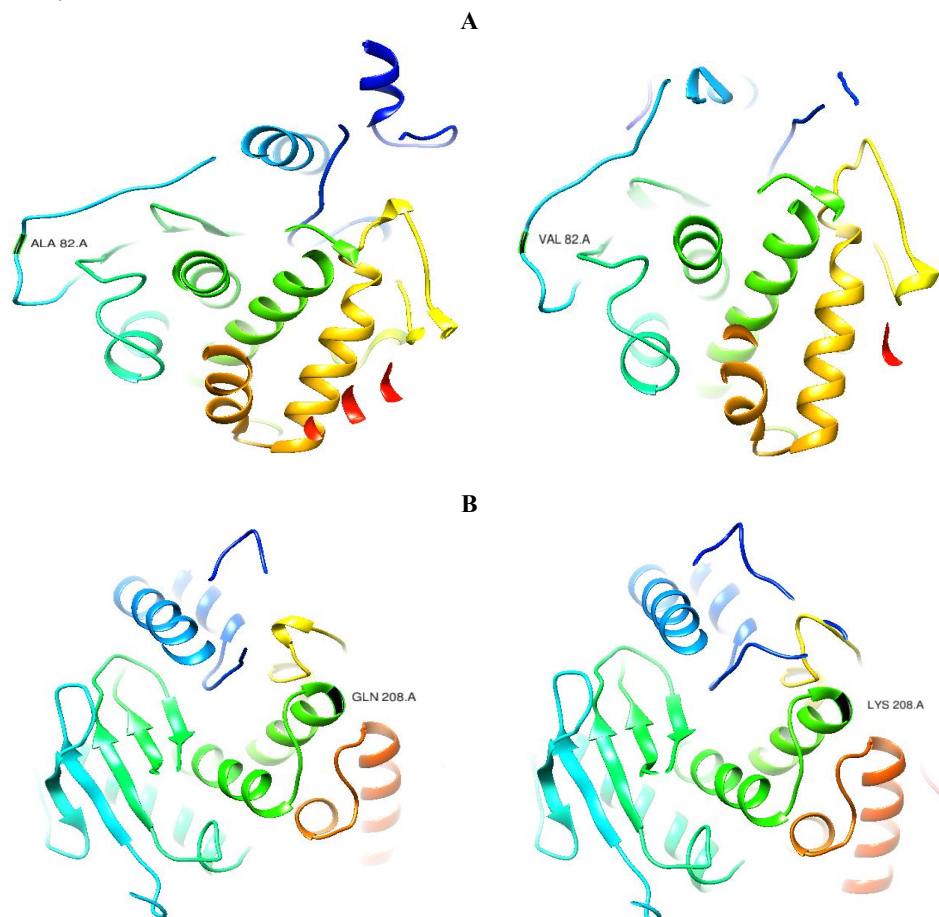


Fig. 11: Amino acid substitution of *MetPr* of: **A;** ALA82VAL and **B;** GLN208LYS in black color, of wild type *S. werraensis* KN23 and mutant *S. werraensis* SA27.

3.7. Docking and molecular interaction studies

One of the most common ways to study drug-receptor interactions and predict how tiny molecules will attach to their target proteins is molecular docking (Karumuri *et al.*, 2015). The

binding method of the substrate beta-keratin to the 3D models of the *serine protease* (*SerPr*) and *metalloprotease* (*MetPr*) proteins was investigated in our work by docking experiments utilizing the HDock online tool. The docking results of ligand beta-keratin with the 3D model of *serine protease* (*SerPr*) revealed the interaction patterns. In the case of the template *S. werraensis* JCM4860 *SerPr*, an affinity score of -266.26 kcal/mol, a confidence score of 0.9109, a ligand RMSD (Å) of 71.53, and active site amino acids of ARG251, PRO252, and TYR264 in the *SerPr* receptor and active site amino acids of LEU71 and VAL76 in the ligand beta-keratin with interface residues of 1.289 and 1.408, respectively, are depicted in figure 12a. In the case of the *S. werraensis* KN23 *SerPr*, an affinity score of -256.51 kcal/mol, a confidence score of 0.8938, a ligand RMSD (Å) of 56.43, and active site amino acids of THR991 and SER1009 in the *SerPr* receptor and active site amino acids of PRO40 and ALA66 in the ligand beta-keratin with interface residues of 2.195 and 2.079, respectively, as depicted in figure 12b, In the case of the mutant *S. werraensis* SA27 *SerPr*, an affinity score of -276.27 kcal/mol, a confidence score of 0.9259, a ligand RMSD (Å) of 54.12, and active site amino acids of SER246 and TRP376 in the *SerPr* receptor and active site amino acids of GLY72 and ALA76 in the ligand beta-keratin with interface residues of 2.1111 and 2.081, respectively, as depicted in figure 12c.

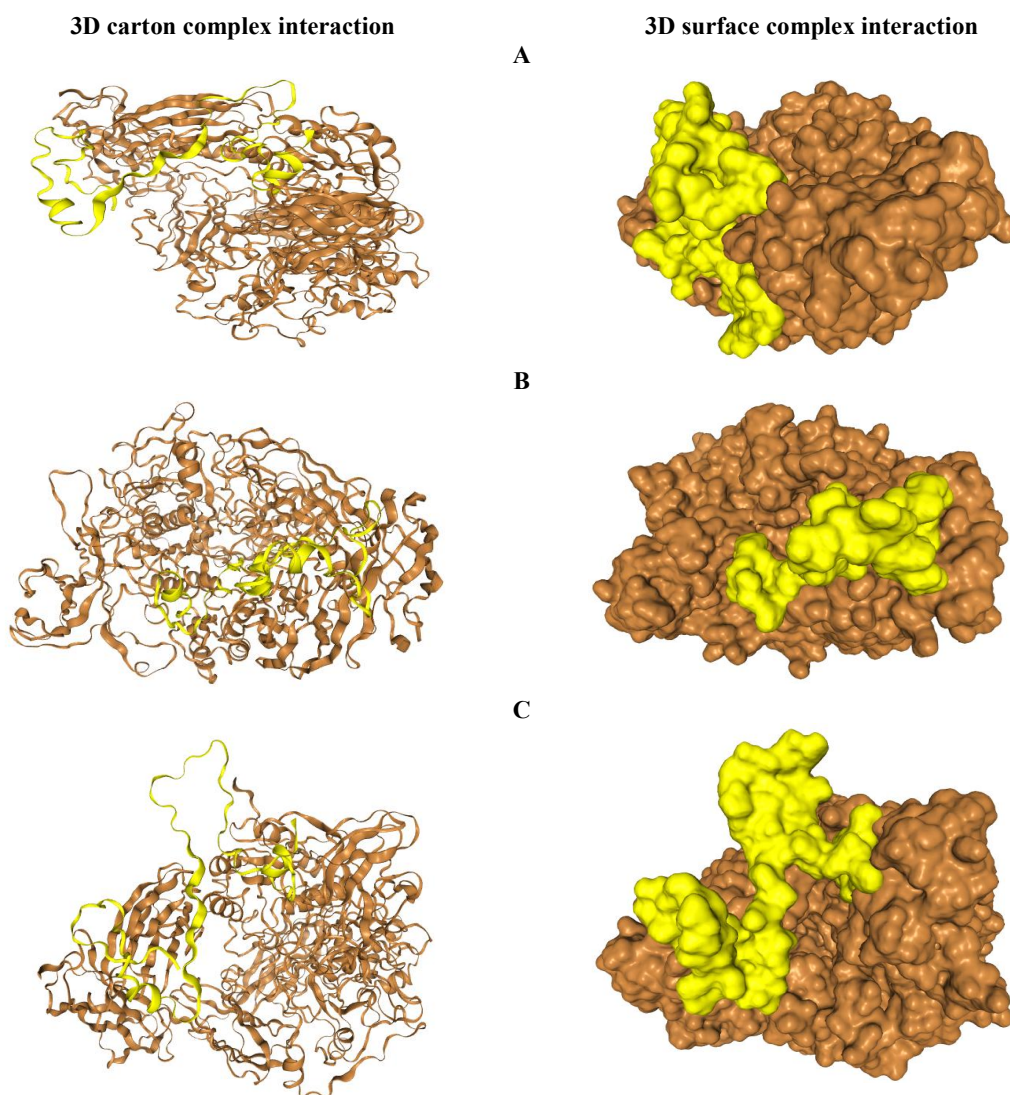


Fig. 12: 3D surface and 3D carton complex interaction showing binding *SerPr* with ligand beta-keratin displaying the most effective binding mode in the protein cavity (active site displayed by yellow colour) of (A) template *S. werraensis* JCM4860; (B) *S. werraensis* KN23; and (C) mutant *S. werraensis* SA27.

The metalloprotease (*MetPr*) 3D model and beta-keratin docking findings showed the interaction patterns. The following factors were considered for the *S. werraensis* JCM 4860 *MetPr* template: an affinity score of -246.86 kcal/mol, a confidence score of 0.8740, a ligand RMSD (Å) of 62.76, and amino acids for the active site of HIS34, ARG 52, ARG 62, and VAL282 in the *MetPr* receptor and active site amino acids of TYR2, GLN37, VAL42, and GLY63 in the ligand beta-keratin with interface residues of 2.079, 2.183, 2.168, and 2.148; respectively, as depicted in figure 13a. In the case of the *S. werraensis* KN23 *MetPr*, an affinity score of -239.16 kcal/mol, a confidence score of 0.8561, a ligand RMSD (Å) of 43.61, and active site amino acids of VAL76 and THR326 in the *MetPr* receptor and active site amino acids of ALA57 and TYR77 in the ligand beta-keratin with interface residues of 0.956 and 1.956; respectively, are depicted in figure 13b. In the case of the mutant *S. werraensis* SA27 *MetPr*, an affinity score of -250.72 kcal/mol, a confidence score of 0.8823, a ligand RMSD (Å) of 34.48, active site amino acids of HIS202 and GLN332 in the *MetPr* receptor, and active site amino acids of ASP3 and CYS13 in the ligand beta-keratin with interface residues of 2.095 and 2.203; respectively, as depicted in figure 13c,

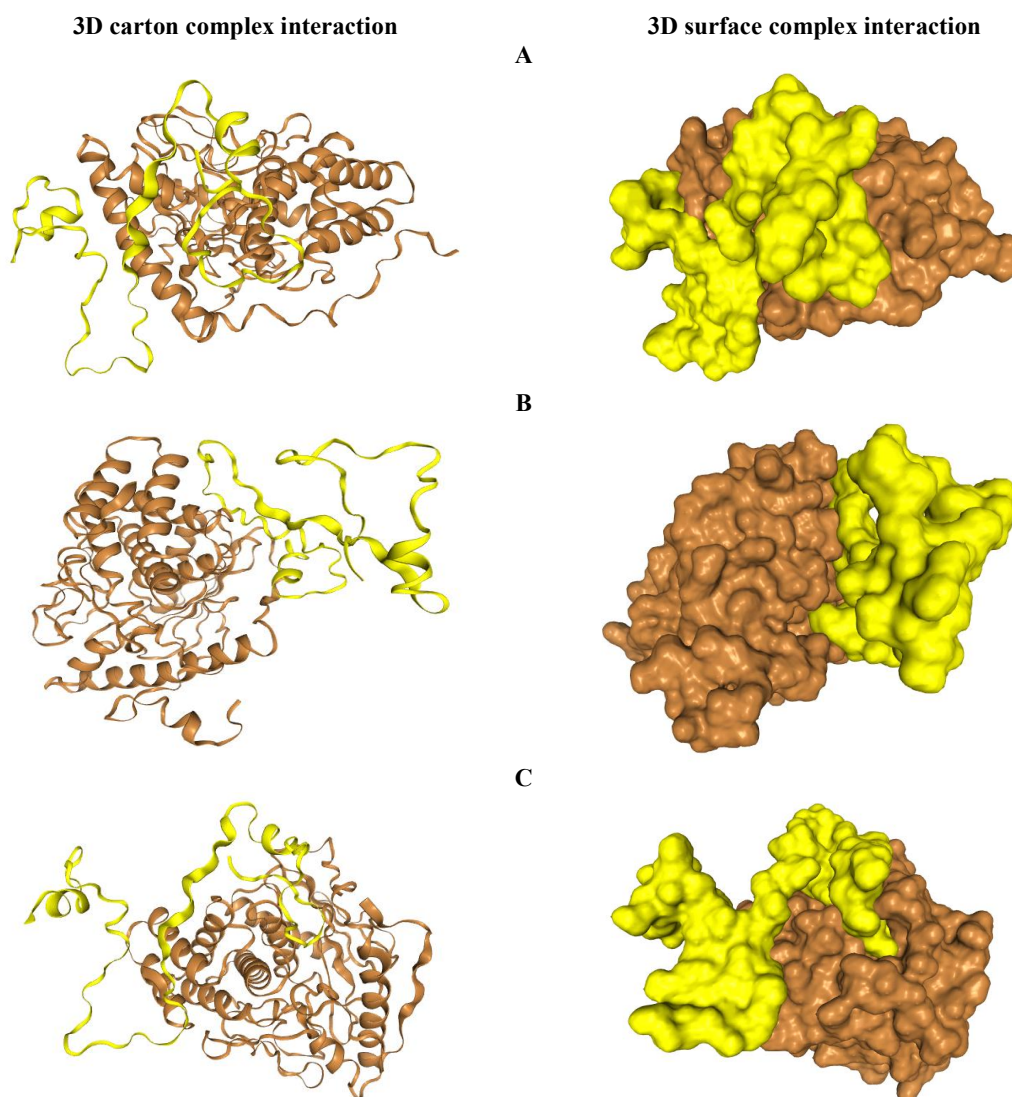


Fig. 13: 3D surface and 3D cartoon complex interaction showing binding *MetPr* with ligand beta-keratin displaying the most effective binding mode in the protein cavity (active site displayed by yellow colour) of (A) template *S. werraensis* JCM4860; (B) *S. werraensis* KN23; and (C) mutant *S. werraensis* SA27.

The catalytic efficiency of keratinases derived from *Bacillus licheniformis* and *Stenotrophomonas sp.* is being investigated. has also been improved using docking studies (Banerjee *et al.*, 2014; Fang *et al.*, 2016). In another study by Gupta *et al.* (2017) when comparing psoriasis drugs, the following drugs were found to have the best binding affinities in the docking studies conducted using the extra precision (XP) method of Glide for the cloned keratinase-encoding gene of *Bacillus subtilis* RSE163: Acitretin (-39.62 kcal/mol), Clobetasol propionate (-37.90 kcal/mol), Fluticasone (-38.53 kcal/mol), Desonide (-32.23 kcal/mol), Anthralin (-38.04 kcal/mol), Calcipotrene (-21.55 kcal/mol), and Mometasone (-28.40 kcal/mol). In another investigation conducted by Banerjee *et al.* (2014) phenylmethylsulfonyl fluoride (PMSF) was used in molecular docking studies to predict the active site of *Bacillus licheniformis alkaline serine protease*. The results showed 100% sequence similarity with the sequence structure of the chosen *Bacillus* genus. Two of the ten docking sites that were found were anticipated to be active sites for the *Bacillus* genus keratinase. Fang *et al.* (2016) reported that *Stenotrophomonas sp.* keratinase docking increases their catalytic efficiency. Patni *et al.* (2021), carried out protein-protein docking: pyDock was used to model the interaction between PE_PGRS39 and the SH3 domain and integrins. Molecular docking was also carried out. Using three integrins with PDB codes, docking was carried out: 4m76 (β 2 integrin; score: -129.39), 4o02 (β 3 integrin; score: -122.25), and 3vi3 (α 5 β 1). Of these, α 5 β 1 displayed the highest affinity (total binding energy) of -138.678. Rahimnahal *et al.* (2023), KRLr1-FK4 docking reports were then submitted, and KRLr1-FK12 structures were added to the HADDOCK server for docking. The KRLr1-FK4 and KRLr1-FK12 complexes' HADDOCK statistical results were contrasted. Comparing the HADDOCK Scores of the KRLr1-FK4 and KRLr1-FK12 complexes, the clusters with the highest negative binding energy were chosen. LRRk1 could interact with FK4 (-130.7 \pm 1.5kcal/mol) with a larger negative energy than FK12 (-111.1 \pm 22kcal/mol), according to the overall HADDOCK data. Almahasheer *et al.* (2022), compared to the predicted structure in its natural state (with an affinity of -6.57 and a score of -6.68 kcal/mol), docking studies revealed that substitutions had an effect on the overlaid structure and resulted in an increased binding of the mutant D137N of KerS13uv+ems (with an affinity of -7.17 and a score of -6.54 kcal/mol) as well as seven mutants of KerS26uv (with an affinity of -7.43 and a score of -7.17 kcal/mol). (Abd El-Aziz *et al.*, 2023b) the molecular docking studies revealed that beta-keratin and the metalloprotease (*MetPr*) had the most binding affinity. *Pichia kudriavzevii* YK46 had a value of -257.02 kcal/mol while *Pichia kudriavzevii* strain 129 had a value of -260.75 kcal/mol. (Abd El-Aziz *et al.*, 2023c) in a molecular docking investigation, the *Rhodotorula mucilaginosa* KR *endo-PGI* template interacted with active sites 1, 2, and 3, respectively, while scoring -6.0, -5.9, and -5.6 kcal/mol for affinity. *Rhodotorula mucilaginosa* PY18 *endo-PGI* had affinity values of -5.8, -6.0, and -5.0 kcal/mol for active sites 1, 2, and 3, correspondingly. Mutant *Rhodotorula mucilaginosa* E54 *endo-PGI* exhibited binding strengths of -5.6, -5.5, and -5.4 kcal/mol for active sites 1, 2, and 3, correspondingly.

3.8. Cloning of serine protease (*SerPr*) and metalloprotease (*MetPr*) encoding genes in *E. coli* DH5a

Researchers investigation serine protease (*SerPr*) and metalloprotease (*MetPr*) encoding gene have a length of 3318 and 1119 bp from *S. werraensis* KN23 (GenBank: OK086273) and mutant *S. werraensis* SA27, and it enhanced by the use of primers that are unique to the gene of interest. An analysis of the PCR results was performed using gel electrophoresis, which revealed the presence of two products measuring 3.318 and 1.119 kilobases (kb) in length, respectively, derived from genomic DNA. From what we can tell, the optimal circumstances for amplifying the target DNA amplicon were achieved at an annealing temperature of 55°C. The Qiagen gel purification kit was used to remove the DNA band of the mutant *S. werraensis* SA27 from the agarose gel. After that, a ligation cloning kit was used to clone it into the pGEM®-T Easy Vector. The cloning was done under T7 and SP6 strong promoters to enable the expression of serine protease (*SerPr*) and metalloprotease (*MetPr*), as shown in figure 14a. The recombinant plasmid obtained was designated as pGEM-T-*SerPr* and pGEM-T-*MetPr*. The recombinant plasmid was introduced into the host organism for protein synthesis, *E. coli* DH5a, using the heat-shock method. The next step was to find transformants that could withstand ampicillin by using the white/blue screening approach, which included IPTG and X-gal. Different transformants derived from the *E. coli* strain were successfully produced by efficient transformation. The plasmids were extracted from *E. coli* transformants that were chosen at random

and then subjected to analysis using agarose gel electrophoresis. PCR amplification was used to screen *E. coli* transformants containing genes for *serine protease (SerPr)* and *metalloprotease (MetPr)*. Specific primers utilized for the isolation of *SerPr* and *MetPr*, as seen in Figures 14b and 14c, were employed for this purpose.

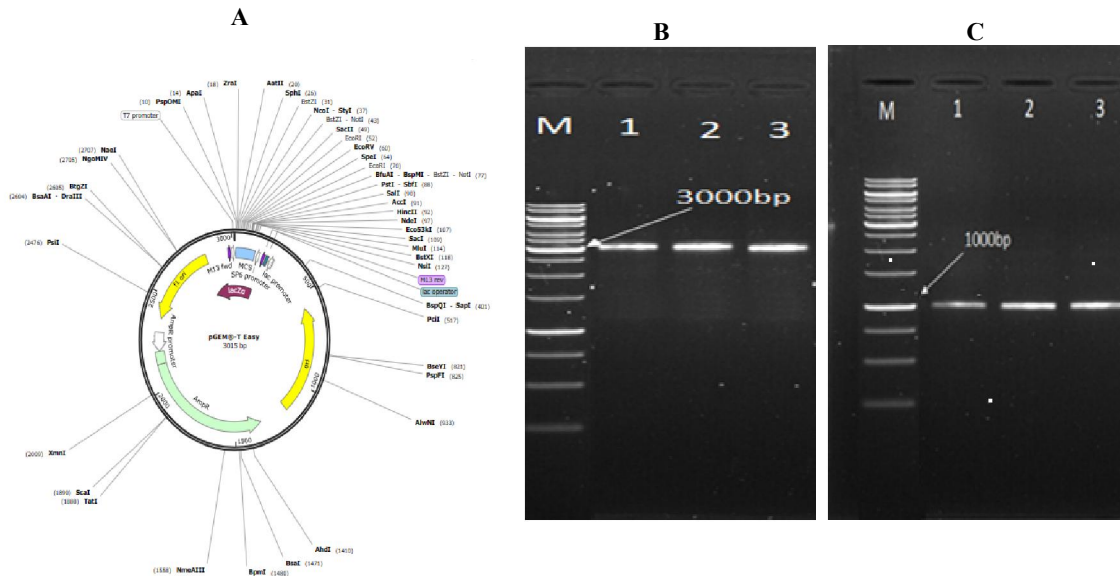


Fig 14: A; pGEM-Teasy cloning vector, Agarose gel electrophoresis of B; lan 1,2 and 3 amplified PCR *SerPr* (3318 bp) of recombinant *pGEM- SerPr- SA27*; C; lan 1,2 and 3 amplified PCR *MetPr* (1119 bp) of recombinant *pGEM- MetPr- SA27*; M, 10.000 bp DNA ladder (Invitrogen, California, USA).

3.9. Keratinolytic *Serine protease (SerPr)* and *metalloprotease (MetPr)* expression

The keratinolytic (*SerPr* and *MetPr*) activity of mutant *S. werraensis* SA27 was conducted by using a fermentation medium that was enhanced with 1% feather as the only carbon source. The experiment included examining the *E. coli* recipient strains, the donor mutant *S. werraensis* SA27, and four *E. coli* strains harboring the *SerPr* and *MetPr* plasmids (*E. coli (pGEM-T-SerPr* and *pGEM-T-MetPr)*). The cultures were placed in an incubator at a temperature of 37°C and subjected to shaking at a speed of 120 revolutions per minute for a maximum duration of 4 days. Each culture was sampled and the obtained supernatant was obtained using centrifugation. This supernatant was used as the crude enzyme for the keratinase activity test, following the previously described method. The findings revealed that the donor mutant *S. werraensis* SA27 had *SerPr* and *MetPr* activity, but the recipient strains of *E. coli* showed no activity. Nevertheless, the *E. coli* cultures that obtained the *SerPr* and *MetPr* plasmids (*E. coli (pGEM-T-SerPr* and *pGEM-T-MetPr)*) exhibited *SerPr* and *MetPr* functionality. The results validated the biological functionality of the cloned *SerPr* and *MetPr* genes. Both *E. coli* recombinant strains exhibited *SerPr* and *MetPr* activity increase with the increase of incubation period with feather. The activity peak was observed on fourth day of incubation, with approximately 193.25 and 211.32 U/mL for *E. coli* DH5α *pGEM-T-SerPr* and *E. coli* DH5α *pGEM-T-MetPr*, respectively, as shown in figure 15. In contrast, the wild-type mutant *S. werraensis* SA27 displayed an activity of 106.92 U/mL on day 3 of incubation, as reported by Abd El-Aziz *et al.* (2023a).

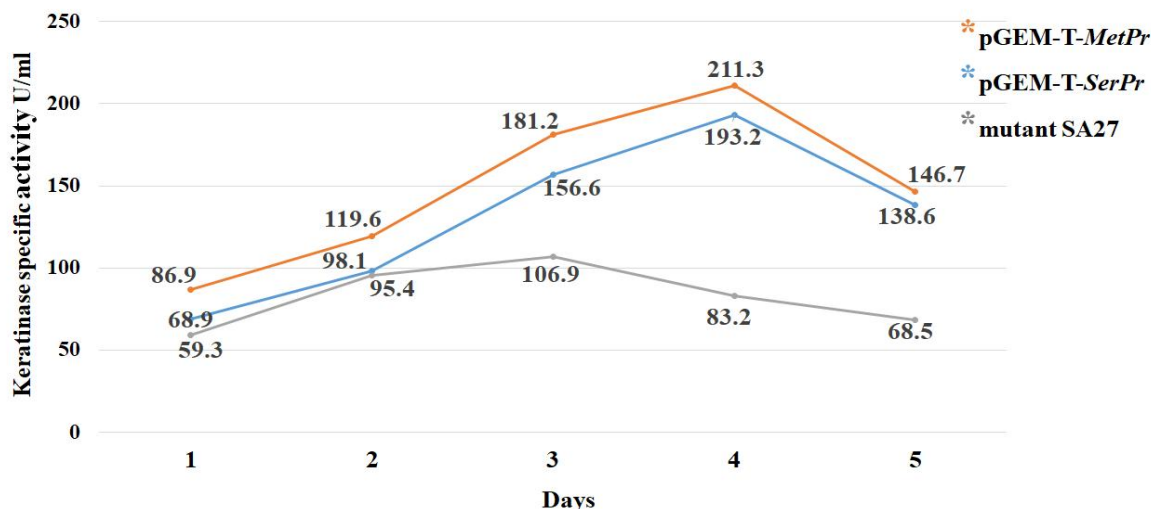


Fig. 15: Keratinolytic *SerPr* and *MetPr* specific activity U/mg protein of recombinant *E. coli DH5α* pGEM-T-*SerPr* and *E. coli DH5α* pGEM-T-*MetPr* begin with 1, 2, 3, 4 and 5 days incubation.

Several studies have concentrated on cloning and expressing keratinases from different native hosts, such as *Bacillus spp.*, *Streptomyces spp.*, *P. aeruginosa*, *A. viridilutea*, *Fervidobacterium sp.*, and *Thermophilus sp.*, to improve the production of recombinant keratinases or to investigate possible improvements. Cloning and expression of these keratinases have also been carried out in many heterologous hosts, including *Escherichia coli*, *Bacillus subtilis*, and *Pichia pastoris* (Nnolim *et al.*, 2020; Baghban *et al.*, 2019). Nevertheless, the current manufacturing of recombinant keratinases remains inadequate to meet large-scale requirements (Nnolim and Nwodo 2021). In a study by Nahar *et al.*, (2016), According to the research, *Bacillus licheniformis* MZK-05 reduced an amplicon of 1,156 base pairs that was aimed squarely at the *kerA* gene, which codes for the keratinase enzyme. Subsequently, the amplicon was replicated into the plasmid vector pGEX-6p-2 for the purpose of expressing it in *Escherichia coli* BL21. The aforementioned expression resulted in a substantial augmentation in keratinolytic activities, measuring 196 U/mL, which signifies an enhanced efficacy of the keratinase. Gupta *et al.* (2017) put the cloned RSE163 keratinase gene from *Bacillus subtilis* into expression. The *ker* gene showed a much higher keratinase activity, measured at 450 ± 10.43 U, when it was expressed in *E. coli*. In, Peng *et al.* (2020) the keratinase gene, which originates in *Bacillus licheniformis* BBE11-1, was effectively expressed in *Bacillus subtilis* WB600. Specifically, they were able to increase the activity level of the recombinant keratinase KerZ1 to 45.14 KU/ml by screening ribosome-binding sites and altering the promoter. Rahimnahal *et al.*, 2023 in one study, the Keratinase gene was successfully expressed in *Escherichia coli* BL21(DE3) using the pET-21b (+) vector. Afterwards, the KRLr1 protein was isolated and purified, yielding 85.96%. The protein was then refolded. In another study, Su *et al.*, 2019 used a genetically modified strain M7 of *B. subtilis* keratinase to produce 3040 U/mL of keratinase outside the cell through 32 hours of continuous fermentation in a 15-liter bioreactor. Wang *et al.*, 2019 the *kerT1* gene, which is 1170 base pairs long, encodes the keratinase enzyme from the feather-degrading bacteria *Thermoactinomyces sp.* YT06. This gene was cloned and expressed in *Escherichia coli* BL21 (DE3). The purification process resulted in obtaining purified recombinant keratinase (rKERTYT) with a yield of 39.16% and a purification factor of 65.27-fold. The specific activity of the purified keratinase was measured to be 1325 U/mg. Mwanza *et al.*, (2021), the target gene of interest was amplified from the genome of *Chryseobacterium carnipullorum* after primer sequences were generated for it. *E. coli* BL21 (DE3) cells were used for cloning, propagation, and expression of the peptidase M64 gene. Liao *et al.*, 2023, reported the production of keratinase from *Bacillus amyloliquefaciens* K11 was effectively adjusted by adjusting the expression components, such as signal peptides and promoters. The optimal result was obtained by combining the signal peptide *SPSacC* with the promoter *Pdual3*, resulting in a 6.21-

fold increase in keratinase activity. In their study, Abd El-Aziz *et al.* (2023b) demonstrated the successful the *MetPr* gene was expressed and cloned in *E. coli* DH5 α . Therefore, keratinase activity skyrocketed, reaching 281 \pm 12.34 U/ml. Abd El-Aziz *et al.*, (2023c), the *endo-PGI* genes were transferred and produced in *E. coli* DH5 α from the yeast strain *Rhodotorula mucilaginosa* PY18 and the mutant *Rhodotorula mucilaginosa* E54. The resultant recombinant *Rhodotorula mucilaginosa* *pGEM-PGI-PY18* had a considerably greater *endo-PGI* activity of 94.57 U/mg, and the recombinant mutant *Rhotorula pGEM-PGI-E54* achieved an even greater *endo-PGI* activity of 153.10 U/mg.

4. Conclusions

Due to the wide range of applications, keratinase had attracted a lot of attention. Novel *Streptomyces werraensis* KN23, an actinomycete strain, was isolated and identified as a potential strain for the synthesis of the keratinase enzyme. The unique *Streptomyces werraensis* KN23 and mutant *Streptomyces werraensis* SA27, which encode *serine protease* (*SerPr*) and *metalloprotease* (*MetPr*) genes, were isolated, sequenced, and submitted to the NCBI GenBank accession number based on the conserved rejoin. The Ramachandran plot, which demonstrated that the residues were accurately modelled, was used to validate the *SerPr* and *MetPr* 3D model. *Streptomyces werraensis* KN23 and mutant *Streptomyces werraensis* SA27 *serine protease* (*SerPr*) and *metalloprotease* (*MetPr*) ultimately exhibited a contact with a high affinity score, according to molecular docking experiments. Mutant *Streptomyces werraensis* SA27 had *serine protease* (*SerPr*) and *metalloprotease* (*MetPr*) expressing genes that were effectively cloned and expressed in *E. coli* DH5 α , yielding greatly elevated levels of keratinase activity. This study's findings highlight the promise of microbial keratinases, especially *SerPr* and *MetPr*, for keratin waste management. Further research in this area may focus on fully characterizing the *SerPr* and *MetPr* proteins, as well as their enzymatic activities. This could include testing its stability in different conditions, ideal pH, and substrate specificity. In addition, to increase the amount and scalability of manufacturing, it is feasible to investigate improving the *SerPr* and *MetPr* expression systems. Other industries that generate keratin waste, such as the textile, leather, and cosmetics industries, may be good candidates for further investigation into the potential applications of *SerPr* and *MetPr*.

List of abbreviations

<i>S. werraensis</i>	<i>Streptomyces werraensis</i>
<i>SerPr</i>	<i>Serine protease</i>
<i>MetPr</i>	<i>Metalloprotease</i>
LB	Luria–Bertani medium
P.C	Plate Count
DMSO	Dimethyl Sulfoxide
TCA	Trichloroacetic Acid
PCR	Polymerase Chain Reaction
NCBI	National Center for Biotechnology Information
C-score	Confidence Score
MOE	Molecular Operating Environment
Amp	Ampicillin
BLAST	Basic Local Alignment Search Tool
ORF	Open Reading Frame
MSA	Multiple Sequence Alignment
EMBL	European Molecular Biology Laboratory
MEGAX	Molecular Evolutionary Genetics Analysis
I-TASSER	Iterative threading assembly refinement
Template Modeling score	TM-score
RMSD	Root Mean Square Deviation
IPTG	Isopropyl β -D-1-thiogalactopyranoside
X-gal	5-bromo-4-chloro-3-indolyl- β -D-galactopyranoside

Acknowledgments:

We thank the National Research Centre, Cairo Egypt for his continuous help.

Author Contributions:

Data analysis, statistical analysis, and data visualization were all a part of the process, and all of the writers had equal say in coming up with the idea for the study, designing it, and doing the experiments. Each portion of the article was written, revised, and edited by them. In addition, the final version of the essay has been reviewed and approved by all writers.

Funding:

Not applicable.

Availability of data and materials

All data generated or analyzed during this study are included in this article.

Data Availability Statement:

The identified *S.werraensis* KN23 sequences have been submitted and can be found in the NCBI database with the accession numbers OK086273. Additionally, serine protease (*SerPr*) and metalloprotease (*MetPr*) from *Streptomyces werraensis* KN23 and mutant *Streptomyces werraensis* SA27 submitted to the NCBI GenBank database accession numbers OR464168, OR464169, OR464170, OR464171. All other relevant data that support the results and conclusions of this study are provided within the article itself.

Declarations

Ethics approval:

Not applicable.

Consent to publication:

Not applicable.

Competing interests

The authors declare that they have no competing interests

References

- Abd El-Aziz, N.M., B.E. Khalil, and H.F. Ibrahim, 2023a. Enhancement of feather degrading keratinase of *Streptomyces swerraensis* KN23, applying mutagenesis and statistical optimization to improve keratinase activity. *BMC microbiology*, 23(1): 158.
- Abd El-Aziz, N.M., B.E. Khalil, and N.N. El-Gamal, 2023b. Structure prediction, docking studies and molecular cloning of novel *Pichia kudriavzevii* YK46 metalloprotease (*MetPr*) for improvement of feather waste biodegradation. *Scientific Reports*, 13(1): 19989.
- Abd El-Aziz, N.M., M.E. Moharam, N.N. El-Gamal, and B.E. Khalil, 2023c. Enhancement of novel *Endo-polygalacturonase* expression in *Rhodotorula mucilaginosa* PY18: insights from mutagenesis and molecular docking. *Microbial Cell Factories*, 22(1): 1-23.
- Abdel-Naby, M.A., W.M. El-Wafa, and G.E. Salim, 2020. Molecular characterization, catalytic, kinetic and thermodynamic properties of protease produced by a mutant of *Bacillus cereus*-S6-3., *Int. J. Biol. Macromol.* 160: 695–702.
- Alexandratos, N., and J. Bruinsma, 2012. World Agriculture Towards 2030/2050: The 2012 Revision. ESA Work. Pap. No. 12–03. Food Agric. Organ, Rome.
- Almahasheer, A.A., A. Mahmoud, H. El-Komy, A.I. Alqosaibi, S. Aktar, S. AbdulAzeez, and J.F. Borgio, 2022. Novel feather degrading keratinases from *Bacillus cereus* group: biochemical, genetic and bioinformatics analysis. *Microorganisms*, 10(1): 93.
- Baghban, R., S. Farajnia, M. Rajabibazl, Y. Ghasemi, and A. Mafi, 2019. Yeast expression systems: overview and recent advances. *Mol. Biotechnol.*, 61:365–384.

- Banerjee, A., D.K. Sahoo, H. Thatoi, B.R. Pati, K.C. Mondal, A. Sen, and P.K. Mohapatra, 2014. Structural characterization and active site prediction of bacterial keratinase through molecular docking., *J. Bioinform.*, 4:67–82.
- Barman, D.N., M.D.A. Haque, S.M.D.A. Islam, H.D. Yun, and M.K. Kim, 2014. Cloning and expression of ophB gene encoding organophosphorus hydrolase from endophytic *Pseudomonas sp.* BF1-3 degrades organophosphorus pesticide chlorpyrifos. *Ecotoxicology and Environmental Safety*, 108: 135–141.
- Beg MA, Shivangi, Thakur SC, Meena LS. 2018. Structural prediction and mutational analysis of Rv3906c gene of *Mycobacterium tuberculosis* H₃₇Rv to determine its essentiality in survival. *Adv Bioinformatics*. 15:6152014.
- Cai, C., B. Lou, and X. Zheng, 2008. Keratinase production and keratin degradation by mutant strain of *Bacillus subtilis*. *J. Zhejiang Univ. Sci. B*, 9(1):60–67.
- Callegaro, K., A. Brandelli, and D.J. Daroit, 2019. Beyond plucking: feathers bioprocessing into valuable protein hydrolysates. *Waste Manag.* 95: 399–415.
- De Oliveira Martinez, J.P.; Cai, G.; Nachtschatt, M.; Navone, L.; Zhang, Z.; Robins, K.; Speight, R. 2020. Challenges and opportunities in identifying and characterising keratinases for value-added peptide production. *Catalysts*, 10, 184.
- Degryse, B., J. Fernandez-Recio, V. Citro *et al.*, 2008. In silico docking of urokinase plasminogen activator and integrins., *BMC Bioinform.*, 9:1–9.
- Eswar N, Webb B, Marti-Renom MA, Madhusudhan MS, Eramian D, Shen MY, Pieper U, Sali A. 2006. Comparative protein structure modeling using Modeller. *Curr Protoc Bioinformatics*. Oct;Chapter 5:Unit-5.6.
- Fang, Z., J. Zhang, B. Liu, G. Du, and J. Chen, 2016. Enhancement of the catalytic efficiency and thermostability of *Stenotrophomonas sp.* keratinase KerSMD by domain exchange with KerSMF. *Microb. Biotechnol.*, 9:35–46.
- Froger, A., and J.E. Hall, 2007. Transformation of plasmid DNA into *E. coli* using the heat shock method. *Journal of Visualized Experiments*, (6): 253.
- Gradišar, H., J. Friedrich, I. Križaj, and R. Jerala, 2005. Similarities and specificities of fungal keratinolytic proteases: comparison of keratinase of *Paecilomycesmarquandii* and *Doratomycesmicrosporusto* some known proteases. *Appl. Environ. Microbiol.*, 71(7):3420–3426.
- Gupta, S., P. Tewatia, J. Misri, and R. Singh, 2017. Molecular modeling of cloned *Bacillus subtilis* keratinase and its insinuation in psoriasis treatment using docking studies. *Indian J. Microbiol.*, 57(4):485–491.
- Heo, L., H. Park, and C. Seok, 2013. GalaxyRefne: protein structure refinement driven by side-chain repacking., *Nucleic Acids Res.*, 41:384–388.
- Huang, Y., P.K. Busk, F.A. Herbst, and L. Lange, 2015. Genome and secretome analyses provide insights into keratin decomposition by novel proteases from the non-pathogenic fungus *Onygena corvina*. *Appl. Microbiol. Biotechnol.* 99: 9635–9649.
- Intagun, W., and W. Kanoksilapatham, 2017. A review: biodegradation and applications of keratin degrading microorganisms and keratinolytic enzymes, focusing on thermophiles and thermostable serine proteases. *Am. J. Appl. Sci.* 14: 1016–1023.
- Karumuri, S., P.K. Singh, and P. Shukla, 2015. In silico analog design for terbinafine against *Trichophyton rubrum*: a preliminary study. *Indian J. Microbiol.*, 55:333–340.
- Kasperova, A., J. Kunert, and M. Raska, 2013. The possible role of dermatophyte cysteine dioxygenase in keratin degradation. *Med. Mycol.* 51: 449–454.
- Kathwate, G.H., 2020. In silico design and characterization of multi epitopes vaccine for SARS-CoV2 from its Spike proteins., *bioRxiv* 56:1115–1135.
- Kesharwani, R.K., and K. Misra, 2011. Prediction of binding site for curcuminoids at human topoisomerase II a protein; an in silico approach. *Curr. Sci.*, 101:1060–1065.
- Kulkarni, P.A., and R.M. Devarumath, 2014. In silico 3D-structure prediction of SsMYB2R: a novel MYB transcription factor from *Saccharum spontaneum*. *Indian J. Biotechnol.*, 13:437–447.
- Lange, L., Y. Huang, and P.K. Busk, 2016. Microbial decomposition of keratin in nature—a new hypothesis of industrial relevance. *Appl. Microbiol. Biotechnol.* 100: 2083–2096.

- Lee, Y.J., H. Jeong, G.S. Park, Y. Kwak, S. Lee, L. Jae, J. Sang, M.K. Park, J.Y. Kim, H.K. Kang, J.H. Shin, and D.W. Lee, 2015b. Genome sequence of a native-feather degrading extremely thermophilic *Eubacterium*, *Fervidobacterium islandicum* AW-1. *Stand. Genomic Sci.* 10: 1–9.
- Li, Z., C. Reimer, M. Picard, A.K. Mohanty, and M. Misra, 2020. Characterization of chicken feather biocarbon for use in sustainable biocomposites. *Front. Mater.* 7: 1–12.
- Liao, Y., M. Xiong, Z. Miao, A.R. Ishaq, M. Zhang, B. Li, Y. Zhan, D. Cai, Z. Yang, J. Chen, and S. Chen, 2023. Modular Engineering to Enhance Keratinase Production for Biotransformation of Discarded Feathers, *Applied Biochemistry and Biotechnology*, 195(3): 1752-1769.
- Maha, T.H.E., 2017. Genetic improvement of bacterial xylanase production., A thesis submitted in partial fulfillment of the requirement for the degree of Doctor of Philosophy in agricultural sciences (genetics). Department of genetics, Faculty of agriculture, Ain Shams University, Egypt.
- Marcos, E., T.M. Chidyausiku, A.C. McShan, T. Evangelidis, S. Nerli, L. Carter, L.G. Nivón, A. Davis, G. Oberdorfer, K. Tripsianes, N.G. Sgourakis, and D. Baker, De novo design of a non-local beta- sheet protein with high stability and accuracy. 2018, *Nature Structural & Molecular Biology*, 25(11): 1028–1034.
- Mei, P.Y., Y. Chie, R. Zhai, and Y. Liu, 2013. Cloning, purification and biochemical properties of a thermostable pectinase from *Bacillus halodurans* M29. *Journal of Molecular Catalysis B: Enzymatic*, 94: 77-81.
- Mercer, D.K., and C.S. Stewart, 2019. Keratin hydrolysis by dermatophytes. *Med. Mycol.* 57: 13–22.
- Mwanza, E.P., W.A. van der Westhuizen, C.E. Boucher, G. Charimba, and C. Hugo, Heterologous expression and characterisation of a keratinase produced by *chryseobacterium carnipullorum*. 2021, *Protein Expression and Purification*, 186: 105926.
- Nahar, M., S. Asaduzzaman, W. Sumaia, H. Sanowarul, I. Mohammad, M.K. Muhammad, N.K. Shakila, H. Mozammel, 2016. Cloning, expression and structure simulation of keratinase from *Bacillus licheniformis* strain MZK05., *Malaysian Journal of Microbiology*, 12(2):182-190.
- Nnolim, N.E. and U.U. Nwodo, 2021. Microbial keratinase and the bioeconomy: a three-decade meta-analysis of research exploit., *AMB Express*, 11:1-16.
- Nnolim, N.E., A.I. Okoh, and U.U. Nwodo, 2020a. *Bacillus* sp. FPF-1 produced keratinase with high potential for chicken feather degradation. *Molecules*, 25:150.
- Ouled-Haddar, H., T.I. Zaghoul, and H.M. Saeed, 2010. Expression of alkaline proteinase gene in two recombinant *Bacillus cereus* featherdegrading strains. *Folia Microbiologia*, 55(1):23-27.
- Patni, K., P. Agarwal, A. Kumar, and L.S. Meena, 2021. Computational evaluation of anticipated PE_PGRS39 protein involvement in host–pathogen interplay and its integration into vaccine development., *3 Biotech*, 11(204):1-17.
- Peng, Z., J. Zhang, Y. Song, R. Guo, G. Du, and J. Chen, 2021. Engineered pro-peptide enhances the catalytic activity of keratinase to improve the conversion ability of feather waste. *Biotechnology and Bioengineering*, 118(7): 2559-2571.
- Peng, Z., X. Mao, J. Zhang, G. Du, and J. Chen, 2020. Biotransformation of keratin waste to amino acids and active peptides based on cell-free catalysis. *Biotechnology for biofuels*, 13(1): 1-12.
- Rahimnahal, S., A. Meimandipour, J. Fayazi, K.A. Asghar, M. Shamsara, N.M. Beigi, H. Mirzaei, M.R. Hamblin, H. Tarrahimofrad, H. Bakherad, J. Zamani and Y. Mohammadi, 2023. Biochemical and molecular characterization of novel keratinolytic protease from *Bacillus licheniformis* (KRLr1), *Front. Microbiol.* 14:1132760. doi: 10.3389/fmicb.2023.1132760
- Roy, A., J. Yang, and Y. Zhang, 2012. COFACTOR: an accurate comparative algorithm for structure-based protein function annotation., *Nucleic Acids Res.*, 40:471–477
- Sahi, S., P. Tewatia, and B.K. Malik, 2012. Modeling and simulation studies of human b3 adrenergic receptor and its interactions with agonists., *Curr. Comput. Aided Drug. Des.*, 8:283–295.
- Shavandi, A., T.H. Silva, A.A. Bekhit, and A.E.D.A. Bekhit, 2017. Keratin: dissolution, extraction and biomedical application. *Biomater. Sci.*, 5: 1699–1735.
- Singh, K.D., and K. Muthusamy, 2013. Molecular modeling, quantum polarized ligand docking and structure-based 3D-QSAR analysis of the imidazole series as dual AT1 and ETA receptor antagonists. *Acta Pharmacol. Sin.*, 34:1592–1606.

- Verma, A., H. Singh, S. Anwar, A. Chattopadhyay, K.K. Tiwari, S. Kaur, and G.S. Dhilon, 2017. Microbial keratinases: industrial enzymes with waste management potential. *Crit. Rev. Biotechnol.*, 37: 476–491.
- Wang, L., Y. Zhou, Y. Huang, Q. Wei, H. Huang, and C. Guo, 2019. Cloning and expression of a thermostable keratinase gene from *Thermoactinomyces* sp. YT06 in *Escherichia coli* and characterization of purified recombinant enzymes., *World Journal of Microbiology and Biotechnology*, 35(9):135.
- Waterhouse, A., M. Bertoni, S. Bienert, G. Studer, G. Tauriello, R. Gumienny, F.T. Heer, T.A.P. de Beer, C. Rempfer, L. Bordoli, R. Lepore, and T. Schwede, 2018. SWISS-MODEL: Homology modelling of protein structures and complexes., *Nucleic Acids Research*, 46(W1): 296–303.
- Wawrzekiewicz, K., J. Lobarzewski, and T. Wolski, 1987. Intracellular keratinase of *Trichophyton gallinae*. *Med. Mycol.*, 25(4):261-268.
- Webb B, Sali A. 2016. Comparative Protein Structure Modeling Using MODELLER. *Curr Protoc Bioinformatics*. Jun 20;54:5.6.1-5.6.37.
- Yahaya, R.S.R., Y.M. Normi, L.Y. Phang, S.A. Ahmad, J.O. Abdullah, and S. Sabri, 2021. Molecular strategies to increase keratinase production in heterologous expression systems for industrial applications., *Applied microbiology and biotechnology*, 105: 3955-3969.
- Yang, J., and Z. Yang, 2015. I-TASSER server: new development for protein structure and function predictions, *Nucleic Acids Res.*, 43: W174–W181.
- Zhang, Y., 2008. I-TASSER server for protein 3D structure prediction., *BMC Bioinform.*, 9:1–8.
- Zheng, W., C. Zhang, Y. Li, R. Pearce, E.W. Bell, and Y. Zhang, 2021. Folding non-homology proteins by coupling deep-learning contact maps with I-TASSER assembly simulations. *Cell Reports Methods*, 1: 100014.